10 Radiogenic Isotopes

The geologic time scale gave a focus to efforts to determine the duration of geologic time. There were a variety of qualitative estimates based on physical and geological processes, as understood in the 1800's. But a truly quantitative approach to measurement of geologic time only became possible with the discovery of radioactivity in 1896, and the eventual understanding of radioactive decay processes in the early 1900's.

Armstrong (1991)

From the perspective of applications to geologic systems, we are interested in only those isotopes that show measurable variations relatable to natural process. Such isotopes may be divided into two distinct groups: *radiogenic isotopes* that are produced by radioactive decay of unstable parent nuclides; and *stable isotopes* that do not undergo radioactive decay. Thus, in a closed system, the abundance of a radiogenic isotope, unlike that of a stable isotope, is a function of the time interval over which the decay process has occurred and is the basis of radiometric dating of geologic samples. A radiogenic isotope itself may be radioactive (e.g., ^{226}Ra, an isotope of radium) or stable (e.g., ^{206}Pb, an isotope of lead).

Both radiogenic and stable isotopes are used extensively for gaining insights into geochemical processes. Reliance on isotope ratios for the interpretation of geochemical processes and products is a relatively recent phenomenon, but helped by the development of instruments and techniques for measurement of ultrasmall amounts of isotopes in earth materials, the study of isotopes has turned out to be a rapidly expanding field of research. The main applications of radiogenic isotopes in geochemistry include:

(1) dating of rocks, minerals, and archeological artifacts (radiometric geochronology);
(2) tracing geochemical processes such as the evolution of the Earth's oceans, crust, mantle, and atmosphere through geologic time, and magmatic differentiation and assimilation (DePaolo and Wasserburg, 1979; DePaolo, 1981);
(3) tracing the sources and transport paths of dissolved and detrital constituents involved in the formation of rocks and mineral deposits (e.g., Hemming *et al.*, 1995, 1996; Capo *et al.*, 1998; Kamenov *et al.*, 2002; Panneerselvam *et al.*, 2006).

In this chapter we will discuss some of these applications of radiogenic isotopes, with emphasis on techniques of radiometric dating. More elaborate treatments of the subject can be found, for example, in Faure (1986, 2001), Dickin (1995), and Banner (2004).

10.1 Radioactive decay

10.1.1 Abundance and stability of nuclides

Only about 430 of approximately 1700 known nuclides occur naturally and of these only about 200 are stable. The stability of a nuclide is a function of the configuration of its nucleus, and the binding energy (per atomic particle), which generally decreases with increasing atomic weight above mass 56. An examination of the atomic structure of the nuclides reveals some interesting general patterns about their stability.

(1) With the exception of only two nuclides, $^{1}_{1}$H and $^{3}_{2}$He, which have fewer neutrons than protons, stable nuclides are characterized by nearly equal numbers of protons (Z)

Introduction to Geochemistry: Principles and Applications, First Edition. Kula C. Misra.

and neutrons (N) (the so-called *symmetry rule*). Actually, the $N : Z$ ratio increases from 1 to about 3 with increasing values of the mass number (A).

(2) Most of the stable nuclides have even numbers of protons and neutrons; stable nuclides with either odd Z or odd N are much less common, and nuclides with odd Z and odd N are rare (the so-called *Oddo–Harkins rule*).

(3) Nuclides that have one of the so-called "magic numbers" (2, 8, 10, 20, 28, 50, 82, and 126) as their Z or N are relatively more stable.

An unstable nuclide decays spontaneously at a constant rate until it is transformed into an isotope with a stable nuclear configuration. *Radioactivity* is this phenomenon of spontaneous decay of unstable nuclides, which are referred to as radioactive nuclides or *radionuclides*, to daughter isotopes. The phenomenon was discovered by the French physicist Henri Becquerel in 1896 but the term "radioactivity" was actually coined by the Polish scientist and Nobel laureate Marie Curie a couple of years later on the basis of ionizing radiation emitted by radium.

Most of the radionuclides that were produced during stellar evolution (see Chapter 12) have become extinct because of their fast decay rates, although they can be produced artificially through nuclear reactions. For geologic applications we are interested in a small group of radionuclides that continue to exist in geologic materials in measurable quantities for one of the following reasons (Banner, 2004):

(1) their decay rates are too slow relative to the age of the Earth (e.g., $^{87}_{37}$Rb, $^{235}_{92}$U);

(2) they are decay products of long-lived, naturally occurring radioactive parents (e.g., $^{222}_{86}$Rn produced from $^{235}_{92}$U);

(3) they are produced naturally as a result of the bombardment of stable isotopes by cosmic rays (e.g., $^{14}_{6}$C from $^{14}_{6}$N);

(4) they are produced by human activities, such as operation of nuclear reactors and testing of nuclear explosions, and released to the environment (e.g., $^{90}_{38}$Sr, $^{239}_{94}$Pu).

10.1.2 *Mechanisms of radioactive decay*

Radioactive decay occurs by three mechanisms: *beta decay*, *alpha decay*, and *spontaneous nuclear fission*, usually accompanied by emission of energy in the form of gamma rays. The alpha/beta/gamma terminology was adopted in the late 1800s, before physicists understood what each of these emissions was made of.

Beta decay

The process of beta decay depends on the ratio of proton (or atomic) number (Z) to neutron number (N) in the radionuclide; in all cases beta decay is accompanied by radiant energy in the form of gamma rays. Radionuclides with an excess of neutrons (i.e., with $N : Z > 1$) decay spontaneously by emitting from the nucleus a negatively charged beta particle or *negatron* (β^-) that is identical in charge and mass to an extranuclear electron. The *negatron decay* may be regarded as the transformation of a neutron into a proton, an electron, which is expelled from the nucleus as a β^- particle, and an *antineutrino* by the reaction

$$\text{neutron} \Rightarrow \text{proton} + \beta^- + \bar{\nu} + \gamma \qquad (10.1)$$

in which energy and mass are conserved as in any chemical reaction. An *antineutrino* ($\bar{\nu}$), an antiparticle of neutrino, is a stable elementary particle that has near zero rest mass and zero electric charge, but its kinetic energy conserves the energy and momentum of the β^- decay nuclear transition. (An *antiparticle* has the same mass as a particle but opposite charge.) The decay produces a new isotope, a *daughter*, in which N is decreased by 1 whereas Z is increased by 1 (Table 10.1). An example is the β^- decay of $^{14}_{6}$C:$^{14}_{6}$C $\Rightarrow$ $_{7}{}^{14}$N + β^- + $\bar{\nu}$ + γ.

For some radionuclides that are deficient in neutrons (i.e., with $N : Z < 1$), beta decay occurs by emission from the nucleus of a positively charged beta particle or *positron* (β^+), which has the same mass as an electron but carries a positive charge. The *positron decay* may be regarded as the transformation of a proton into a neutron that is accompanied by the emission of a positron and a neutrino according to the reaction:

$$\text{proton} \Rightarrow \text{neutron} + \beta^+ + \nu + \gamma \qquad (10.2)$$

A *neutrino* (ν) is a stable elementary particle with variable kinetic energy but with very small (but nonzero) rest mass and zero electric charge; neutrinos conserve the energy and momentum of the positron decay nuclear transition. Neutrinos travel at or close to the speed of light, and are able to pass through ordinary matter almost undisturbed. They are extremely difficult

Table 10.1 Daughter nuclide produced by alpha and beta decay of parent radionuclide.

	Decay mechanism	Atomic number	Neutron number	Mass number
Parent nuclide		Z	N	$A = Z + N$
Daughter nuclide	α^{2+} (alpha) decay	$Z - 2$	$N - 2$	$A - 4$
	β^- (negatron) decay	$Z + 1$	$N - 1$	A
	β^+ (positron) decay	$Z - 1$	$N + 1$	A
	Electron capture decay	$Z - 1$	$N + 1$	A

to detect. The positron decay produces a new isotope in which N increases by 1 whereas Z decreases by 1 (Table 10.1). An example is the β^+ decay of $^{10}_{6}$C: $^{10}_{6}\text{C} \Rightarrow {}^{10}_{5}\text{B} + \beta^+ + \nu + \gamma$.

A third type of beta decay is called *electron capture*. This process involves the spontaneous capture of an electron orbiting close to the nucleus, and transformation of a proton to a neutron and a neutrino (which is ejected from the atom's nucleus) by the reaction:

$$\text{proton} + e^- \Rightarrow \text{neutron} + \nu + \gamma \qquad (10.3)$$

The decay produces a new isotope in which, as in the case of positron decay, N increases by 1 whereas Z decreases by 1 (Table 10.1). An example is the electron capture by $^{11}_{6}$C: $^{11}_{6}\text{C} + e^- \Rightarrow {}^{11}_{5}\text{B} + \nu$. Electron capture is also called K-capture because the captured electron usually comes from the atom's K-shell.

Alpha decay

A large number of radionuclides undergo decay by emission of *alpha particles* from the nucleus. An alpha particle (α^{2+}) is composed of two neutrons and two protons, identical to the nucleus of helium ($^{4}_{2}$He); so both N and Z for the new nuclide formed by *alpha decay* decrease by 2, resulting in a decrease of the atomic mass (A) by 4 (Table 10.1). An example is the alpha decay of $^{238}_{92}$U to $^{234}_{90}$Th: $^{238}\text{U} \Rightarrow {}^{234}\text{Th} + \alpha^{2+} + \text{energy}$.

Nuclear fission

A few of the heaviest isotopes, such as those of uranium and transuranic elements (elements with atomic mass greater than that of uranium), decay by spontaneous *fission*. In this process the nucleus breaks into two or more unequal fragments, accompanied by the release of a large amount of energy. Generally, the fission products have excess neutrons and therefore undergo further decay by β^- and gamma-ray emission until a stable nuclide is formed. The operation of fission nuclear reactors around the world is based on this principle.

Most radionuclides decay by one of the mechanisms described above, the most common being β^- decay. Some isotopes, however, undergo *branched decay* – decay by more than one mechanism simultaneously – each branch producing a different daughter. For example, in a given population of $^{40}_{19}$K atoms, 88.8% decay to stable $^{40}_{20}$Ca atoms by negatron emission and 11.2% decay to stable $^{40}_{18}$Ar atoms by positron emission and electron capture (see section 10.3.5).

10.2 Principles of radiometric geochronology

10.2.1 Decay of a parent radionuclide to a stable daughter

As proposed first by Rutherford and Soddy (1902), the rate of decay of a radioactive nuclide at any instant is proportional to the number of atoms of the nuclide remaining at that instant. Denoting the number of radioactive parent atoms remaining at any time t by N (not to be confused with the neutron number mentioned earlier), the mathematical expression for the rate of radioactive decay (dN/dt), a first-order reaction (see section 9.1.3), can be written as

$$-\frac{dN}{dt} \propto N \quad \text{or} \quad -\frac{dN}{dt} = \lambda N \qquad (10.4)$$

where the negative sign reminds us that N decreases with time, and λ is the proportionality constant, usually called the *decay constant*, which is expressed in units of reciprocal time. The decay constant states the probability that a given atom of the radionuclide will decay within a stated time. Every radioactive decay scheme has its own characteristic numerical value of λ, which is not affected by temperature, pressure, and any chemical changes involving the isotope. The constant rate of radioactive decay over geologic time is the fundamental premise of age dating by radiogenic isotopes.

The integrated form of the rate equation (10.4), as mentioned in section 9.1.3 and elaborated in Box 10.1, is:

Box 10.1 Integrated form of the radioactive decay equation

Integrating equation (10.4), we have

$$\int -\frac{dN}{N} = \int \lambda \, dt = \lambda \int dt$$

$$-\ln N = \lambda t + \text{Integration constant (IC)}$$

Denoting the value of N as N_0 at $t = 0$, $-\ln N_0 = \text{IC}$. Substituting for IC,

$$-\ln N = \lambda t - \ln N_0$$

Rearranging, we get, $-\ln (N/N_0) = \lambda t$, which is commonly expressed as

$$N = N_0 \, e^{-\lambda t} \qquad (10.5)$$

$$\boxed{N = N_0 \, e^{-\lambda t}} \qquad (10.5)$$

where N_0 represents the number of radioactive parent atoms present when the rock or mineral was formed (i.e., at time $t = 0$), t is the time interval (in years) over which radioactive decay has occurred, and N represents the number of radioactive parent atoms remaining after time t. Equation (10.5) describes the basic quantitative relationship among N, N_0, and t for any radioactive decay process of known λ. The decay constant is related to the half-life ($t_{1/2}$) of the decay process – the value of t when $N = 1/2\ N_0$ – by the equation (see section 9.1.3):

$$\boxed{t_{1/2}(\text{yr}) = \frac{0.693}{\lambda\ (y^{-1})}} \qquad (10.6)$$

We can express equation (10.5) in terms of daughter atoms. Let us assume that the radioactive parent produces D^* atoms of a stable daughter during time t. Since the decay of one parent atom produces one daughter atom,

$$D^* = N_0 - N \tag{10.7}$$

Substituting for N (equation 10.5),

$$\boxed{D^* = N_0 - N = N_0 - N_0 e^{-\lambda t} = N_0(1 - e^{-\lambda t})} \tag{10.8}$$

Equation (10.5) describes the time-dependent exponential decay of a known population of parent atoms and equation (10.8) the complementary growth of the stable daughter atoms (Fig. 10.1).

10.2.2 Basic equation for radiometric age determination

The direct application of equations (10.5) and (10.8) to natural geochemical systems, such as samples of rocks and minerals, is limited by our lack of knowledge of N_0. We can, however, circumvent this limitation by expressing N_0 in terms of N and D^*, quantities we can actually measure in the laboratory. Substituting for N_0 in equation (10.7), we get the equation for the growth of the daughter,

$$\boxed{D^* = N_0 - N = Ne^{\lambda t} - N = N(e^{\lambda t} - 1)} \tag{10.9}$$

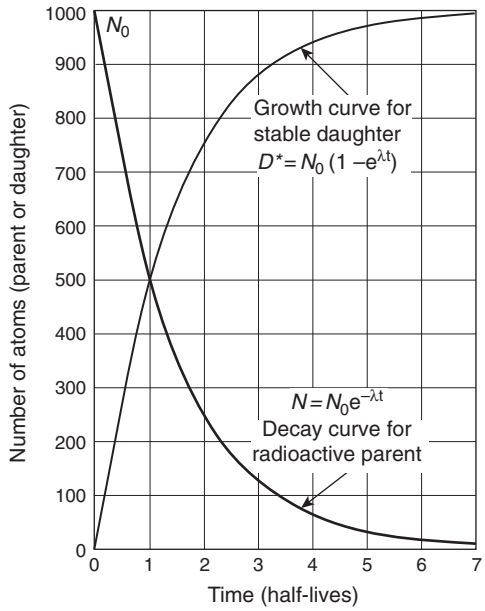

Fig. 10.1 The decay curve for a hypothetical population of 1000 radioactive atoms (N_0) as a function of time expressed in units of half-lives and the complementary growth curve representing the generation of atoms of a stable daughter by radioactive decay (D^*). Both the curves are asymptotic to the time axis.

where t is the geologic age of the sample, and N and D^*, respectively, are the number of parent atoms remaining and the number of the stable daughter atoms generated in time t per unit weight of the sample.

To derive a general equation for isotope-based geochronology, we should also consider the possibility that the system under consideration may have contained some daughter atoms prior to the incorporation of the radioactive parent into the sample. In that case,

$$D = D_0 + D^* \tag{10.10}$$

where D and D_0 represent, respectively, the total number (after time t) and the initial number (at time t_0) of the stable daughter atoms per unit weight of the sample. Substituting for D^* in equation (10.10) we get the basic general equation for age determination of rocks and minerals (Fig. 10.2):

$$\boxed{D = D_0 + N(e^{\lambda t} - 1)} \tag{10.11}$$

which may be rearranged to yield the following expression for t:

$$\boxed{t = \frac{1}{\lambda} \ln \left[\frac{D - D_0}{N} + 1 \right]} \tag{10.12}$$

The quantity D_0 is of interest also because of the information it contains about the history of the daughter before its incorporation into the sample being analyzed.

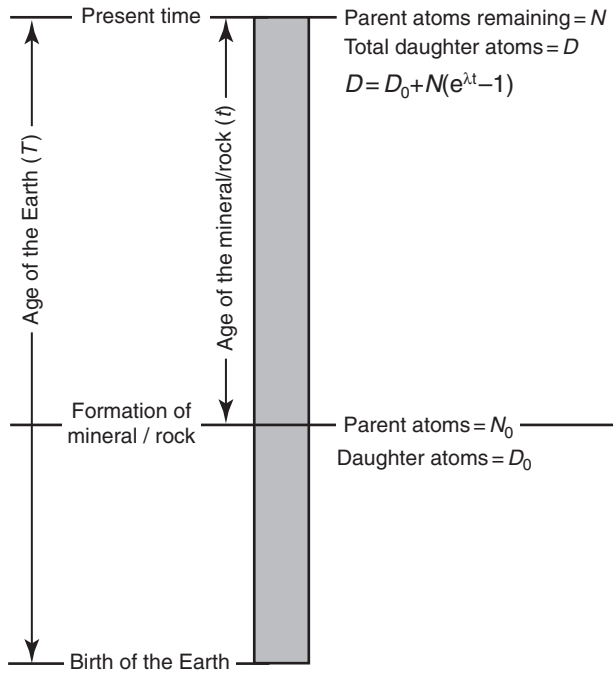

Fig. 10.2 Schematic representation of the geochronologic equation (10.11).

We can use equation (10.12) to calculate t for a mineral or rock sample, provided the following conditions are satisfied (Wetherill, 1956b; Faure, 1986).

(1) The value of λ is known accurately and has not changed over geologic time (for parent nuclides with long half-lives, a small error in λ translates into a large uncertainty in the calculated age).
(2) The measurements of D and N are accurate and representative of the rock or mineral to be dated.
(3) The system has remained closed to the parent, the unstable intermediate daughters, and the stable daughter since the formation of the mineral or rock t years ago; i.e., the D^*/N ratio in the sample has changed since that time only as a result of radioactive decay, not by any gain or loss of either the parent or the daughter. Commonly, this is the most difficult condition to satisfy.
(4) It must be possible to assign a realistic value to D_0. This is accomplished either by analyzing several cogenetic (i.e., with same t and D_0) samples (see Fig. 10.4) or by assuming a value based on experience with the particular decay scheme and samples. The latter is not a particularly desirable approach, but the error introduced due to an incorrect value of D_0 is relatively small if the samples chosen for geochronology are highly radiogenic (i.e., $D^* >> D_0$).

Conditions (3) and (4) define a model for the geologic history of the sample. The date calculated from equation (10.12) is commonly referred to as the *model age* because the determined age is valid only to the extent that the actual geologic history of the sample used conforms to the assumed model defined by conditions (3) and (4).

As ratios of isotope abundances can be measured more accurately in the laboratory than absolute abundances, the basic practical equation for geochronology is obtained by dividing both sides of equation (10.11) by the abundance of a nonradiogenic isotope that has remained constant in the samples of interest through geologic time. For example, for the decay of $^{176}_{71}$Lu to $^{176}_{72}$Hf ($^{176}_{71}\text{Lu} \Rightarrow {}^{176}_{72}\text{Hf} + \beta^- + \bar{\nu}$ + energy), where Q represents the output energy), the equation incorporating the nonradiogenic isotope $^{177}_{72}$Hf takes the form

$$\frac{^{176}\text{Hf}}{^{177}\text{Hf}} = \left(\frac{^{176}\text{Hf}}{^{177}\text{Hf}}\right)_0 + \frac{^{176}\text{Lu}}{^{177}\text{Hf}}\,(e^{\lambda t} - 1) \qquad (10.13)$$

where $(^{176}\text{Hf}/^{177}\text{Hf})_0$ is the initial ratio, and ^{176}Hf/^{177}Hf and ^{176}Lu/^{177}Hf are the present-day ratios in the sample of interest. Note that the ratios in this equation (and other geochronologic equations) are atomic ratios.

Radioactive decay schemes commonly used for age dating of earth materials are listed in Table 10.2, and a few of the systems are discussed in section 10.3. In all cases, isotope ratios are measured with a mass spectrometer, an instrument designed to separate charged atoms and molecules of different masses based on their motions in electrical and/or magnetic

Table 10.2 Radioactive decay schemes commonly used for geochronology.

Parent / daughter pair	Decay mechanism	λ (yr^{-1})*	(a) Half-life (yr) (b) Effective range for geochronology (yr)	Typical samples
^{238}U / ^{206}Pb	Decay chain $8\alpha^{2+} + 6\beta^-$	1.55×10^{-10}	(a) 4.47×10^9 (b) $T - 10^7$	Zircon, badellyite, uraninite, monazite, Pb-bearing minerals
^{235}U / ^{207}Pb	Decay chain $7\alpha^{2+} + 4\beta^-$	9.85×10^{-10}	(a) 7.04×10^8 (b) $T - 10^7$	Zircon, badellyite, uraninite, monazite, Pb-bearing minerals
^{232}Th / ^{208}Pb	Decay chain $6\alpha^{2+} + 4\beta^-$	4.95×10^{-11}	(a) 1.40×10^{10} (b) $T - 10^7$	Zircon, badellyite, uraninite, monazite, Pb-bearing minerals
^{87}Rb / ^{87}Sr	β^-	1.42×10^{-11}	(a) 4.88×10^{10} (b) $T - 10^7$	K-feldspar, mica, whole rock
^{40}K / ^{40}Ar	Electron capture	5.81×10^{-11}	(a) 1.19×10^{10} (b) $T - 10^3$	Sanidine, hornblende, plagioclase, mica, whole rock
^{147}Sm / ^{143}Nd	α^{2+}	6.54×10^{-12}	(a) 1.06×10^{11} (b) $T - 0$	Pyroxene, amphibole, feldspars, whole rock
^{14}C / ^{14}N	β^-	1.21×10^{-4}	(a) 5.73×10^3 (b) 70, 000 – 0	Charcoal, wood, peat
^{176}Lu / ^{176}Hf	β^-	1.94×10^{-11}	(a) 3.57×10^{10}	Apatite, zircon, garnet, monazite, whole rock
^{187}Re / ^{187}Os	β^-	1.64×10^{-11}	(a) 4.23×10^{10}	Molybdenite, osmiridium, laurite

*Ages reported in the older literature may have been based on slightly different values of decay constants, and should be recalculated using the decay constants given above. T = age of the Earth.
Sources of data: compilations by Faure (1986), Dickin (1995), Brownlow (1996), and Banner (2004).

fields. The reader may refer to Faure (1986, pp. 56–63) for a succinct discussion of mass spectrometry used in isotope geochemistry.

10.2.3 Decay series

The formulations presented in the previous section presume a one-step, direct decay of a parent radionuclide into a stable daughter. This, however, is not always the case. Some radionuclides, such as ^{238}U, ^{235}U, and ^{232}Th, decay to a stable daughter through a series of short-lived, radioactive daughter isotopes. For example, the decay of ^{238}U into the stable daughter ^{206}Pb occurs through 14 intermediate isotopes of 8 different elements (Fig. 10.3). The chain involves both α and β^- decay and branches repeatedly, but all possible paths lead to ^{206}Pb, the stable isotope of lead. One of the decay products in the ^{238}U decay series is radon gas (^{222}Rn), which is colorless and odorless, but radioactive with a half-life of 3.83 days. Radon gas is chemically inert, but it is a potential health hazard because both radon and its intermediate decay products, isotopes of polonium (Po), are radioactive. When humans inhale radon gas or its radioactive decay products, polonium particles stick to the lungs' bronchi, where they decay by emitting α particles in all directions. Some of the α particles hit the cells lining the bronchi, and may cause cell mutation and ultimately lung cancer in some cases.

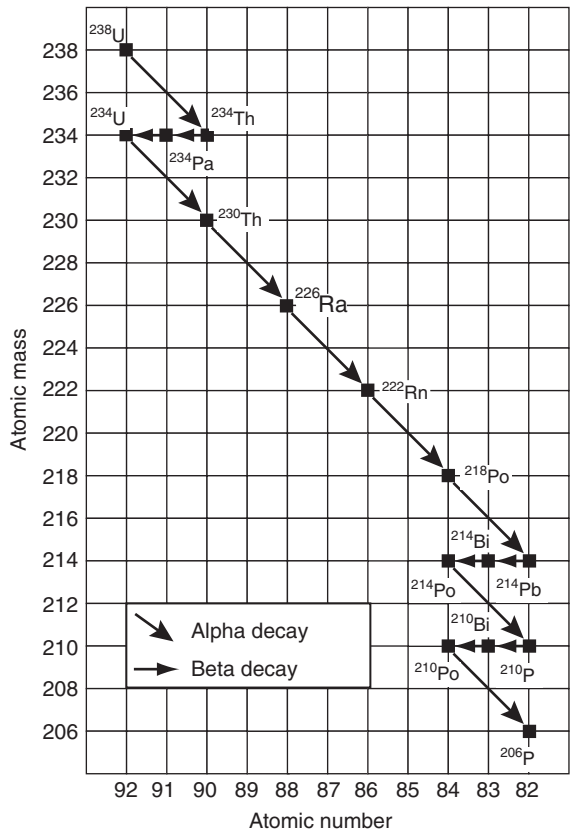

Fig. 10.3 Uranium-238 decay series: the radioactive decay of parent $^{238}_{92}$U nuclide (half-life = 4.47×10^9 yr) to its stable daughter nuclide $^{206}_{82}$Pb via a series of intermediate radiogenic daughters, including radium ($^{226}_{88}$Ra; half-life = 1622 yr) and radon gas ($^{222}_{86}$Rn; half-life = 3.83 days).

Consider a decay series comprised of N_A atoms of a parent A decaying to N_B atoms of a radioactive daughter B, which then decays to N_C atoms of a second radioactive daughter C, and so on to N_S atoms of a stable daughter S. Let λ_A, λ_B, λ_C, … represent the corresponding decay constants. If λ_A is much smaller than the decay constants of the intermediate daughters (i.e., the parent has a much longer half-life compared to the daughters), then it can be shown that (see, e.g., Faure, 1986)

$$\lambda_A N_A = \lambda_B N_B = \lambda_C N_C = \ldots \tag{10.14}$$

and

$$N_S = N_A(e^{\lambda_A t} - 1) \tag{10.15}$$

This condition, in which the rate of decay of the daughter nuclide is equal to that of its parent nuclide, is known as *secular equilibrium*. When a decay series has achieved secular equilibrium, the system can be treated as though the initial parent decayed directly to the stable daughter without intermediate daughters. Thus, equation (10.11) (which is identical to equation 10.15) is valid, for example, for a ^{238}U (parent) ⇒ ^{206}Pb (stable daughter) system that has achieved secular equilibrium.

10.3 Selected methods of geochronology

10.3.1 Rubidium–strontium system

Rubidium has two naturally occurring isotopes – radioactive $^{87}_{37}$Rb (27.835 atom %) and stable $^{85}_{37}$Rb (72.165 atom %) – whereas strontium has four – $^{88}_{38}$Sr (82.58 atom %), $^{87}_{38}$Sr (7.00 atom %), $^{86}_{38}$Sr (9.86 atom %), and $^{84}_{38}$Sr (0.56 atom %), all of which are stable. The Rb–Sr dating method is based on the β^- decay of ^{87}Rb to ^{87}Sr in Rb-bearing minerals and rocks ($\lambda_{Rb} = 1.42 \times 10^{-11}\,\text{yr}^{-1}$; $T_{1/2\,(Rb)} = 48.8 \times 10^9$ yr). The relevant equation for Rb–Sr geochronology (see equation 10.11), incorporating ^{86}Sr as the nonradiogenic isotope for normalization, is:

$$\boxed{\frac{^{87}\text{Sr}}{^{86}\text{Sr}} = \left(\frac{^{87}\text{Sr}}{^{86}\text{Sr}}\right)_0 + \frac{^{87}\text{Rb}}{^{86}\text{Sr}}\,(e^{\lambda_{Rb} t} - 1)} \tag{10.16}$$

where $(^{87}\text{Sr}/^{86}\text{Sr})_0$, $^{87}\text{Sr}/^{86}\text{Sr}$, and $^{87}\text{Rb}/^{86}\text{Sr}$ denote, respectively, the initial mole ratio, the measured mole ratio, and the present-day mole ratio in the sample, and t is its geologic age.

In principle, equation (10.16) can be solved for t if this is the only unknown variable (see equation 10.12). The $^{87}\text{Sr}/^{86}\text{Sr}$ ratio in a sample is measured with a suitable mass spectrometer,

and the concentrations of Rb and Sr are determined either by X-ray fluorescence or by isotope dilution technique. The ratio of Rb/Sr concentrations is converted to $^{87}Rb/^{86}Sr$ by the following equation (Faure, 1986):

$$\frac{^{87}Rb}{^{86}Sr} = \left(\frac{Rb}{Sr}\right)\left(\frac{\text{abundance of } ^{87}Rb}{\text{abundance of } ^{86}Sr}\right)\left(\frac{\text{atomic wt of Sr}}{\text{atomic wt of Rb}}\right) \tag{10.17}$$

where $^{87}Rb/^{86}Sr$ is the present atomic ratio of the isotopes in a unit weight of the sample, and Rb/Sr is the ratio of concentrations of these elements in unit weight of the sample. The atomic weight and isotopic composition of rubidium is known to be the same at the present time ($^{87}Rb = 27.8346$ atom %) in all samples of terrestrial, meteoritic, and lunar rubidium, but the abundance of ^{86}Sr and the atomic weight of strontium depend on the abundance of ^{87}Sr and therefore appropriate values must be calculated for each sample from measured strontium isotope ratios.

$$^{84}Sr = \frac{\frac{^{84}Sr}{^{88}Sr}}{\Sigma\text{ratios}} = \frac{0.00675}{1.4246} = 0.004738;\ ^{86}Sr = \frac{\frac{^{86}Sr}{^{88}Sr}}{\Sigma\text{ratios}} = \frac{0.1194}{1.4246} = 0.08381$$

$$^{87}Sr = \frac{\frac{^{87}Sr}{^{88}Sr}}{\Sigma\text{ratios}} = \frac{0.2985}{1.4246} = 0.20953;\ ^{88}Sr = \frac{\frac{^{88}Sr}{^{88}Sr}}{\Sigma\text{ratios}} = \frac{1.0000}{1.4246} = 0.70195$$

Abundances of the Sr isotopes expressed as atom %:

$^{84}Sr = 0.474$ $^{86}Sr = 8.381$ $^{87}Sr = 20.953$ $^{88}Sr = 70.195$

Atomic weight of Sr in the sample

$$= \frac{(0.474 \times 83.9134) + (8.381 \times 85.9092) + (20.953 \times 86.9088) + (70.195 \times 87.9056)}{100}$$

$$= \frac{39.775 + 720.005 + 1821.000 + 6170.533}{100} = \frac{8751.313}{100} = 87.513$$

Example 10–1. Calculation of the atomic weight of Sr in a sample from measured Sr isotope ratios (Faure, 1986)

Consider a rock sample in which the Sr isotope ratios have been measured as:

$^{87}Sr/^{86}Sr = 2.5000$ $^{86}Sr/^{88}Sr = 0.11940$ $^{84}Sr/^{88}Sr = 0.006756$

The masses of Sr isotopes are (in amu):

$^{84}Sr = 83.9134$ $^{86}Sr = 85.9092$ $^{87}Sr = 86.9088$
$^{88}Sr = 87.9056$

Let us calculate the atomic weight of Sr in this sample.

$$\frac{^{87}Sr}{^{88}Sr} = \frac{^{87}Sr}{^{86}Sr} \times \frac{^{86}Sr}{^{88}Sr} = 2.500 \times 0.1194 = 0.2985$$

Sum of iotope ratios,

$$\sum \text{ratios} = \frac{^{84}Sr}{^{88}Sr} + \frac{^{86}Sr}{^{88}Sr} + \frac{^{87}Sr}{^{88}Sr} + \frac{^{88}Sr}{^{88}Sr} = 0.006756 + 0.11940 + 0.2985 + 1.0000 = 1.4246$$

Fractional abundances of the Sr isotopes in the sample:

The initial ratio, $(^{87}Sr/^{86}Sr)_0$, can be estimated in various ways. If the mineral to be dated is strongly enriched in radiogenic ^{87}Sr, one can assume a value of $(^{87}Sr/^{86}Sr)_0$ based on experience – for example, an initial ratio of 0.704 for uncontaminated mafic volcanic rocks of recent age derived from the upper mantle – because in such cases the age calculated using equation (10.16) is relatively insensitive to the value of $(^{87}Sr/^{86}Sr)_0$. A more reliable approach is the one proposed by Nicolaysen (1962), which takes advantage of the fact that the form of equation (10.16) is that of a straight line. So, a plot $^{87}Sr/^{86}Sr$ (y axis) against $^{87}Rb/^{86}Sr$ (x axis) for a suite of comagmatic igneous mineral separates and whole-rocks (i.e., all of them are of the same age and can be assumed to have the same value of initial strontium ratio) that span a wide range of Rb:Sr ratios, will ideally define a straight line with y-axis intercept = $(^{87}Sr/^{86}Sr)_0$, and slope $(m) = e^{\lambda_{Rb}t} - 1$ (Fig. 10.4). We can calculate t, which in this case represents the age of magmatic crystallization, from the slope of the line:

$$\boxed{t = \frac{\ln(m+1)}{\lambda_{Rb}}} \tag{10.18}$$

The straight line generated in such a plot is called an *isochron* (iso = equal, chron = time), because all samples having the same age (and the same initial ratio) should plot on this line. In practice, a straight line is fitted to the array of points by a statistical method called linear regression, and a correlation

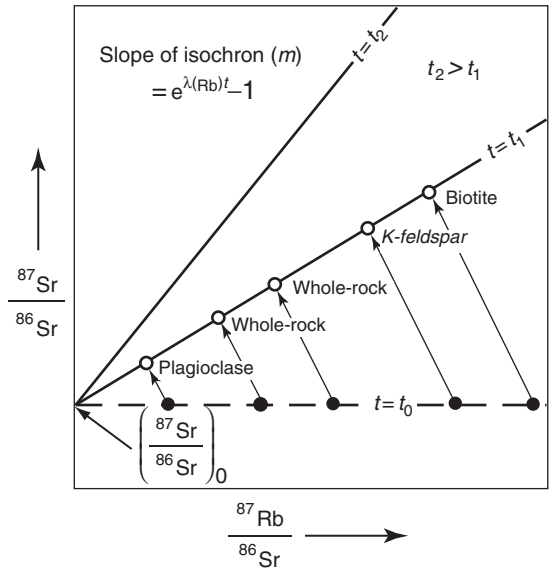

Fig. 10.4 Schematic Rb–Sr isochron diagram for two different suites of comagmatic igneous minerals and whole-rocks. The two suites are of different age (t_1 and t_2) but formed from homogeneous magmas having the same initial strontium ratio. The horizontal line is also an isochron (t_0), representing the time when the minerals and rocks had the same initial ratio and no radiogenic ^{87}Sr. The arrows indicate the generation of radiogenic ^{87}Sr by the decay of ^{87}Rb over the time period t_1. The radiogenic ^{87}Sr is proportional to the ^{87}Rb originally present in the sample. Note that the $(^{87}Sr/^{86}Sr)_0$ of a comagmatic suite can be approximated by the $^{87}Sr/^{86}Sr$ ratio of a sample with a very low concentration of ^{87}Rb.

error is calculated for the isochron (York, 1969; Dickin, 1995). A computer program titled *Isoplot 3.00* (Ludwig, 2003) that runs under Microsoft Excel is also available for such calculations, and can be obtained without charge from Ken Ludwig (kludwig@bgc.org). The opportunity for a statistical treatment of the data to estimate the uncertainty in the determined age is a big advantage of the Rb–Sr and other isochron methods. For example, the age and initial ratio of the Sudbury Nickel Irruptive, the host for the world-famous nickel sulfide deposits, and its initial ratio were determined by Rb–Sr as 1843 ± 133 Ma and 0.7071 ± 0.0005 (Fig. 10.5a).

10.3.2 Samarium–neodymium system

Samarium and neodymium each have seven naturally occurring isotopes. The isotopes, along with their abundances in atom % are: $^{144}_{62}Sm$ (3.1%), $^{147}_{62}Sm$ (15.0%), $^{148}_{62}Sm$ (11.2%), $^{149}_{62}Sm$ (13.8%), $^{150}_{62}Sm$ (7.4%), $^{152}_{62}Sm$ (26.7%), and $^{154}_{62}Sm$ (22.8%); and $^{142}_{60}Nd$ (27.1%), $^{143}_{60}Nd$ (12.2%), $^{144}_{60}Nd$ (23.9%), $^{145}_{60}Nd$ (8.3%), $^{146}_{60}Nd$ (17.2%), $^{148}_{60}Nd$ (5.7%), and $^{150}_{60}Nd$ (5.6%). The Sm–Nd method of age dating is based on the alpha decay of $^{147}_{62}Sm$ to $^{143}_{60}Nd$ ($\lambda_{Sm} = 6.54 \times 10^{-12}\,yr^{-1}$; $t_{1/2}$ (Sm) $= 1.06 \times 10^{11}$ yr). The equation for Sm–Nd geochronology is analogous to that for the Rb–Sr system:

$$\boxed{\frac{^{143}Nd}{^{144}Nd} = \left(\frac{^{143}Nd}{^{144}Nd}\right)_0 + \frac{^{147}Sm}{^{144}Nd}\left(e^{\lambda_{Sm}t} - 1\right)} \qquad (10.19)$$

where ^{144}Nd used for normalization is the nonradiogenic isotope of constant abundance through geologic time, $^{143}Nd/^{144}Nd$ is the measured mole ratio in a sample, $(^{143}Nd/^{144}Nd)_0$ is the initial neodymium ratio, $^{147}Sm/^{144}Nd$ is the present-day mole ratio in unit weight of the sample, and t is the geologic age of the sample. In essence, age determination by the Sm–Nd method is similar to that by the Rb–Sr method, and consists of establishing an isochron in coordinates of $^{143}Nd/^{144}Nd$ (y axis) and $^{147}Sm/^{144}$ Nd (x axis) by analyzing a suite of cogenetic mineral separates or whole rocks (or a combination of the two), and calculating the age from the slope of the isochron (m),

$$m = \left(e^{\lambda_{Nd}t} - 1\right) \qquad (10.20)$$

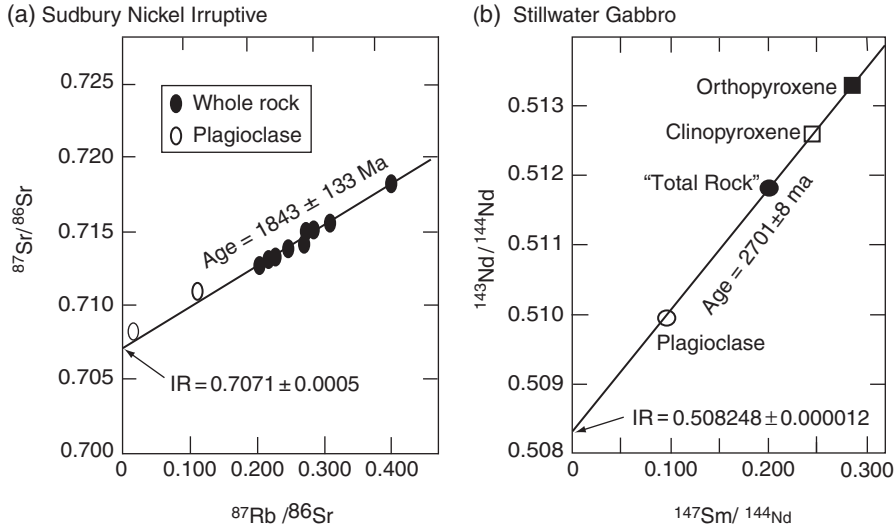

Fig. 10.5 Isochron diagrams. (a) Rb–Sr isochron for the norite unit of the Sudbury Nickel Irruptive (Ontario, Canada) defined by a suite of whole-rock samples of norite and two plagioclase concentrates (Hurst and Farhat, 1977). The age from the slope of the isochron, recalculated to $\lambda(^{87}Rb \Rightarrow {}^{87}Sr) = 1.42 \times 10^{-11}$ by Faure (1986) is 1843 ± 133 Ma, and its y-axis intercept gives an initial $(^{87}Sr/^{86}Sr)$ ratio (IR) of 0.7071 ± 0.0005. (b) Sm–Nd isochron for the Stillwater Layered Complex (Montana, USA). The calculated age from the slope of the isochron is 2701 ± 8 Ma ($\lambda_{Sm} = 6.54 \times 10^{-12}\,yr^{-1}$) and its y-axis intercept gives an initial ratio of 0.508248 ± 0.000012. (Source of data: DePaolo and Wasserburg, 1979.)

or from equation (10.16) after obtaining an estimate of the initial neodymium ratio. For example, the age of the Stillwater Layered Complex was determined as 2701 ± 8 Ma by the Sm–Nd isochron method (Fig. 10.5b; DePaolo and Wasserburg, 1979).

The Sm–Nd method is particularly suitable for dating mafic and ultramafic igneous rocks, whereas the Rb–Sr method is more applicable to dating intermediate and felsic igneous rocks. This is because the Sm : Nd ratios of igneous rocks decrease with increasing degree of differentiation in spite of an increase in the concentrations of both elements. On the other hand, because of the geochemical coherence between Rb and K and between Sr and Ca, the Rb : Sr ratio increases with increasing degree of differentiation. The usefulness of the Sm–Nd system for dating ancient rocks is enhanced by the ability of Sm and Nd to reside in some common rock-forming minerals (e.g., clinopyroxene in komatiites and basalts) and common accessory minerals (e.g., monazite, allanite, titanite, and zircon in granitoids) that are resistant to postcrystallization modification. Thus, the Sm and Nd isotopes remain relatively undisturbed on the whole-rock scale during metamorphism, hydrothermal alteration, or weathering. A limitation of the Sm–Nd method is the lack of a large range of Sm : Nd ratios in natural rocks and minerals owing to the strong geochemical coherence between the two rare earth elements; this limits the precision of absolute age determined from a Sm–Nd isochron.

10.3.3 Uranium–thorium–lead system

Naturally occurring isotopes of the U–Th–Pb system include three radioactive isotopes of uranium [$^{238}_{92}$U (99.2743 atom %), $^{235}_{92}$U (0.7200 atom %), and $^{234}_{92}$U (0.0057 atom %)], only one isotope of thorium ($_{90}{}^{232}$Th) that is radioactive, and four stable isotopes of lead [$^{204}_{82}$Pb (1.4 atom %), $^{206}_{82}$Pb (24.1 atom %), $^{207}_{82}$Pb (22.1 atom %), and $^{208}_{82}$Pb (52.4 atom %)]. The isotope ^{204}Pb has no long-lived radioactive parent, so that its terrestrial abundance may be presumed to have been constant through geologic time. The other three isotopes are radiogenic and their terrestrial abundances have steadily increased throughout geologic time by radioactive decay of parent uranium and thorium nuclides into ^{206}Pb, ^{207}Pb, and ^{208}Pb (Table 10.2). Lead isotopes are commonly measured as ratios relative to nonradiogenic ^{204}Pb, and the corresponding equations for geochronology are:

$$\frac{^{206}\text{Pb}}{^{204}\text{Pb}} = \left(\frac{^{206}\text{Pb}}{^{204}\text{Pb}}\right)_0 + \frac{^{238}\text{U}}{^{204}\text{Pb}}(e^{\lambda_{238}t} - 1) \tag{10.21}$$

$$\frac{^{207}\text{Pb}}{^{204}\text{Pb}} = \left(\frac{^{207}\text{Pb}}{^{204}\text{Pb}}\right)_0 + \frac{^{235}\text{U}}{^{204}\text{Pb}}(e^{\lambda_{235}t} - 1) \tag{10.22}$$

$$\frac{^{208}\text{Pb}}{^{204}\text{Pb}} = \left(\frac{^{208}\text{Pb}}{^{204}\text{Pb}}\right)_0 + \frac{^{232}\text{Th}}{^{204}\text{Pb}}(e^{\lambda_{232}t} - 1) \tag{10.23}$$

where λ_{238}, λ_{235}, and λ_{232} are the decay constants for ^{238}U, ^{235}U, and ^{232}Th, respectively, and the subscript "0" refers to initial ratio. U–Pb age determinations are more accurate when the lead isotopic composition is highly radiogenic because the age calculation then becomes almost independent of the initial lead isotope ratio.

In principle, each of the equations (10.21)–(10.23) can be used to construct an isochron diagram and determine the age of a cogenetic suite of rocks, as we have discussed for the ^{87}Rb – ^{87}Sr method, and the ages so determined should ideally be concordant (that is, $t_{206} = t_{207} = t_{208}$). Smith and Farquhar (1989) applied such an approach (a plot of ^{206}Pb/^{204} Pb versus ^{238}U/^{204}Pb) for direct dating of certain Phanerozoic corals. In practice, however, such an isochron approach does not work for U–Th–Pb systems as the samples analyzed seldom satisfy the critical requirement of having remained closed to U, Th, and Pb (as well as the intermediate daughters) during the lifetime of the system being dated. A way to minimize this problem is to reframe the geochronologic equations in terms of lead isotope ratios (e.g.,^{207}Pb/^{206} Pb). Ratios are likely to be relatively insensitive to lead loss because of geochemical coherence among the lead isotopes. Three widely used dating methods involving lead isotope ratios are briefly discussed below.

U–Pb Concordia diagram

Rearranging equation (10.21), we get

$$\boxed{\frac{^{206}\text{Pb}^*}{^{238}\text{U}} = (e^{\lambda_{238}t} - 1)} \tag{10.24}$$

where ^{206}Pb* represents radiogenic ^{206}Pb produced during the time interval t; that is,

$$\frac{^{206}\text{Pb}^*}{^{238}\text{U}} = \frac{\dfrac{^{206}\text{Pb}}{^{204}\text{Pb}} - \left(\dfrac{^{206}\text{Pb}}{^{204}\text{Pb}}\right)_0}{\dfrac{^{238}\text{U}}{^{204}\text{Pb}}} \tag{10.25}$$

Similarly, equation (10.20) can be rearranged to give

$$\boxed{\frac{^{207}\text{Pb}^*}{^{235}\text{U}} = (e^{\lambda_{235}t} - 1)} \tag{10.26}$$

where ^{207}Pb* represents radiogenic ^{207}Pb produced during the time interval t, and can be expressed by an equation similar to equation (10.25). We can calculate t from equations (10.24) and (10.26) by inserting the measured isotopic composition of a U-bearing mineral into the left-hand side of these equations, provided we can estimate $(^{206}\text{Pb}/^{204}\text{Pb})_0$ and $(^{207}\text{Pb}/^{204}\text{Pb})_0$ or ignore these two terms with justification.

Accessory minerals that have been used for U–Pb dating include zircon ($ZrSiO_4$), badellyite (ZrO_2), monazite ($CePO_4$),

apatite [$Ca_5(PO_4)_3(OH, F, Cl)$], titanite ($CaTiSiO_5$), perovskite ($CaTiO_3$), rutile (TiO_2), allanite (a complex Ca–Mn–Fe–Al silicate of the epidote group), and xenotime (YPO_4). Zircon is by far the most preferred mineral as it has a relatively high concentration of U (because U^{4+} substitutes quite readily for Zr^{4+} due to identical charge and similar ionic radius), is widely distributed (present in most felsic to intermediate igneous rocks), and contains very little initial Pb (because Pb^{2+} does not substitute easily for U^{4+} in the zircon crystal structure). Zircon is extremely resistant to hydrothermal alteration, and can survive diagenesis, metamorphism, or weathering that may modify or destroy its host rock (Amelin *et al.*, 1999; Valley *et al.*, 2005). Zircon crystals with heavy radiation damage or post-magmatic alteration can be identified easily and excluded from analysis. Moreover, the newly developed chemical abrasion ("CA–TIMS") technique involving high-temperature annealing, followed by partial HF digestion at high temperature and pressure, can be effective at removing portions of zircon crystals that have lost Pb, without affecting the isotopic systematics of the remaining material (Mattinson, 2005). The small amounts of initial lead isotopes, $(^{206}Pb)_0$ and $(^{207}Pb)_0$, incorporated in a zircon crystal can be estimated from measurements of the amount of ^{204}Pb in the mineral and $^{206}Pb/^{204}Pb$ and $^{207}Pb/^{204}Pb$ ratios of the whole rock (Dickin, 1995). The estimated amounts of $(^{206}Pb)_0$ and $(^{207}Pb)_0$ are subtracted from the present-day ^{206}Pb and ^{207}Pb values to yield the amounts of radiogenic ^{206}Pb and ^{207}Pb in the zircon. Another advantage of using zircon crystals is that they may be zoned (Fig. 10.6), the different zones representing separate events such as magmatic crystallization or metamorphism. In such cases, the zones, which must be treated as different populations, may provide a chronology of successive events experienced by the host rock.

If a uranium-bearing mineral behaves as a closed system, equations (10.24) and (10.26) should, in principle, yield concordant ages. In reality, however, even zircon crystals often yield discordant ages because of some Pb loss from the system of interest. In some such cases it may still be possible to interpret the isotopic data by means of the *concordia* diagram devised by Wetherill (1956a). The concordia curve is constructed by plotting compatible values of $^{206}Pb^*/^{238}U$ (y axis) against $^{207}Pb^*/^{235}U$ (x axis) calculated for chosen values of t (Fig. 10.7), so that every point on the concordia corresponds to a particular value of t, if the system can be presumed to have been closed to U, Pb, and the intermediate daughters. Any U–Pb system that plots on the concordia yields concordant dates, which can be calculated from the coordinates of the point on the concordia; any U–Pb system that does not, yields discordant dates – i.e., the age calculated using equation (10.24) is not the same as that calculated using equation (10.26).

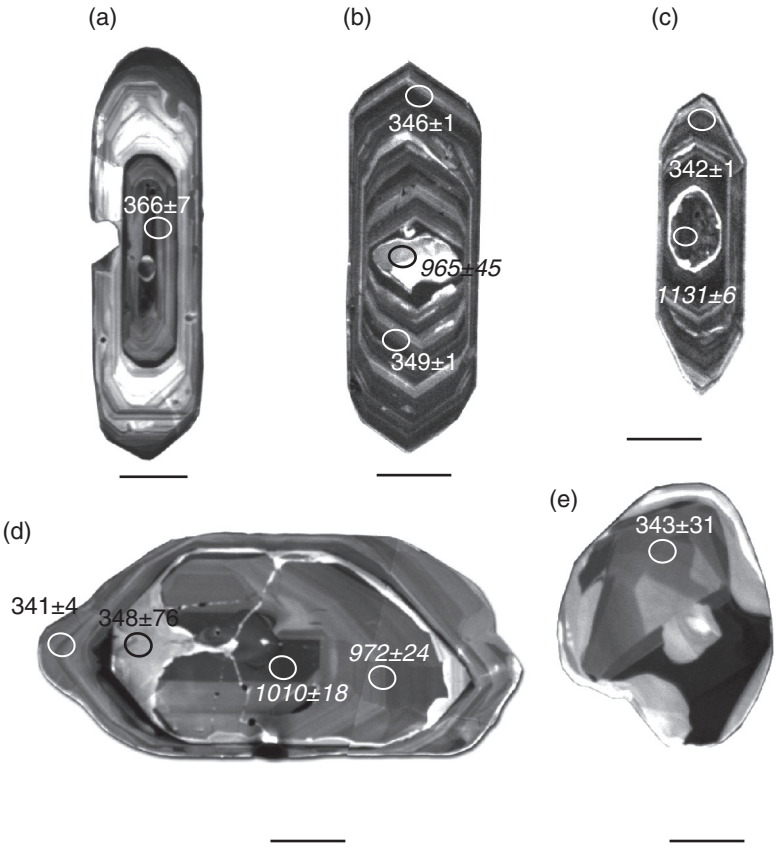

Fig. 10.6 Cathodoluminescence images of zoned zircon crystals showing radiometric ages (SHRIMP-RG analyses) at different spots. Italicized numbers are Pb/Pb ages, all others are $^{206}Pb/^{238}U$ ages. Circular black spots are mineral inclusions. Each scale bar is 100 μm. (a) Magmatic zircon with oscillatory growth zoning (Byars, 2009). (b and c) Magmatic zircons with oscillatory growth zoning and inherited cores (Stahr, 2007). (d) Detrital zircon with faintly zoned, roughly concentric metamorphic rim overgrowths (Merschat, 2009). (e) Soccerball metamorphic zircon with sector zoning (Merschat, 2009). (Compiled by Arthur Merschat, Department of Earth and Planetary Sciences, The University of Tennessee, Knoxville.)

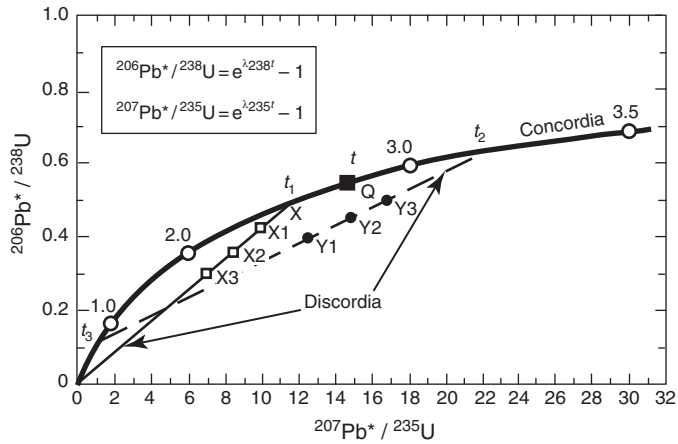

Fig. 10.7 U–Pb concordia diagram illustrating interpretations of lead isotopic data for uranium-bearing minerals such as zircon. The concordia is generated by plotting $^{206}Pb^*/^{238}U$ against $^{207}Pb^*/^{235}U$, which are calculated for selected values of t (a few of which are marked on the concordia), using equations (10.22) and (10.24). For a zircon plotting on the concordia (e.g., point Q), an identical age (t) can be calculated from either of the equations. For discordant zircon crystals that experienced an episode of Pb loss (or U gain) to varying degrees, represented by the points X1, X2, and X3 on the discordia passing through the origin, the crystallization age (t_1) is given by the point X on the Concordia. For the discordia defined by zircons of the same age but variable degrees of Pb loss (points Y1, Y2, and Y3), the upper intersection of the discordia with the concordia gives the age of zircon crystallization (t_2). The lower intersection (t_3) is the age of the lead-loss event if the lead loss was episodic; it has no age significance if the Pb loss was by continuous diffusion over a long period of time.

Let us consider a population of cogenetic zircon crystals of age t_1 whose isotopic composition is represented by point X on the concordia (Fig. 10.7). Suppose that the zircon population experienced an episode of Pb loss resulting from metamorphism or hydrothermal alteration, and that the lead lost had the same isotopic composition as the total lead that was in the mineral (a condition not likely to be satisfied if lead was added to the mineral). It seems that Pb is more easily lost from crystals of small size, crystals containing high concentration of U, or crystals with a high degree of radiation damage. With variable loss of Pb, the changed isotopic compositions of the zircon crystals would lie on a straight line joining point X and the origin of the concordia diagram (the coordinates of any zircon crystal from which all the radiogenic Pb has been lost). Such a chord is called a *discordia* because U–Pb systems lying on it yield discordant dates. Discordant zircons that have lost varying degrees of U as a result of chemical weathering recently may also lie on a discordia that passes through the origin but they should plot above the concordia. In general, this graphical procedure will not be applicable where lead has been added to a U–Pb system unless the isotopic composition of the added lead is known.

In some cases, zircon crystals separated from a single rock (e.g., a granite) plot on a discordia that intersects the concordia at two points (Fig. 10.7). The upper intercept represents the crystallization age of zircon (t_2). Assuming that the Pb loss was instantaneous, the lower intercept is interpreted as the age (t_3) of the event that disturbed the system (Wetherill, 1956b); the intercept has no age significance if the Pb was lost by continuous diffusion over a long period of time. Additional geological information would be required to distinguish between episodic and continuous Pb loss models for a given set of samples. The computer code *Isoplot* (version 3.00) by Ludwig (2003) can be used for constructing the concordia, statistical fitting of discordias to analytical data, and calculating the coordinates of the points of intersection with the concordia.

Isotopic composition of lead in U- and Th-bearing minerals and whole rocks

An equation relating the isotopic composition of lead in U- and Th-bearing minerals to model age can be obtained by combining equations (10.21) and (10.22) and substituting for the present-day $^{238}U/^{235}U$ ratio, which is equal to 137.88:

$$\frac{\dfrac{^{207}Pb}{^{204}Pb} - \left(\dfrac{^{207}Pb}{^{204}Pb}\right)_0}{\dfrac{^{206}Pb}{^{204}Pb} - \left(\dfrac{^{206}Pb}{^{204}Pb}\right)_0} = \frac{^{235}U}{^{238}U}\left(\frac{e^{\lambda_{235}t} - 1}{e^{\lambda_{238}t} - 1}\right) = \frac{1}{137.88}\left(\frac{e^{\lambda_{235}t} - 1}{e^{\lambda_{238}t} - 1}\right) \tag{10.27}$$

Usually, we write this equation in a more compact form as

$$\boxed{\frac{^{207}Pb^*}{^{206}Pb^*} = \frac{^{235}U}{^{238}U}\left(\frac{e^{\lambda_{235}t} - 1}{e^{\lambda_{238}t} - 1}\right) = \frac{1}{137.88}\left(\frac{e^{\lambda_{235}t} - 1}{e^{\lambda_{238}t} - 1}\right)} \tag{10.28}$$

where $^{207}Pb^*/^{206}Pb^*$ refers to the ratio of the two lead isotopes produced by radioactive decay during time t.

Equation (10.27) indicates that a suite of closed U–Pb systems having the same age and the same initial lead isotopic composition should form a straight line array in a plot of $^{207}Pb/^{204}Pb$ (y axis) versus $^{206}Pb/^{204}Pb$ (x axis), the measured present-day ratios in the samples. This straight line, an isochron, will pass through a point whose coordinates are $(^{207}Pb/^{204}Pb)_0$ and $(^{206}Pb/^{204}Pb)_0$, and its slope (m) will be given by:

$$\boxed{\text{slope } (m) = \frac{1}{137.88}\left(\frac{e^{\lambda_{235}t} - 1}{e^{\lambda_{238}t} - 1}\right)} \tag{10.29}$$

Evidently, the slope of the isochron depends only on the age t, which in turn is determined by the isotopic composition of lead in the samples (and does not require any knowledge of the U and Pb concentrations in the samples), and can be determined from the equation of the regression line fitted to the data points. Equation (10.29) is transcendental (i.e. it cannot be solved for t by algebraic methods) and therefore has to be solved by an

Table 10.3 Calculated values of slopes (m) of isochrons for selected values of model age (t), using equation (10.29)

t (Ga)	Slope (m)	t (Ga)	Slope (m)	t (Ga)	Slope (m)
0.1	0.04801	1.6	0.09872	3.1	0.23701
0.2	0.05011	1.7	0.10419	3.2	0.25242
0.3	0.05233	1.8	0.11004	3.3	0.26897
0.4	0.05470	1.9	0.11629	3.4	0.28674
0.5	0.05722	2.0	0.12299	3.5	0.30583
0.6	0.05990	2.1	0.13015	3.6	0.32635
0.7	0.06276	2.2	0.13782	3.7	0.34840
0.8	0.06580	2.3	0.14604	3.8	0.37211
0.9	0.06904	2.4	0.15483	3.9	0.39760
1.0	0.07250	2.5	0.16426	4.0	0.42502
1.1	0.07619	2.6	0.17437	4.1	0.45451
1.2	0.08012	2.7	0.18520	4.2	0.48624
1.3	0.08432	2.8	0.19682	4.3	0.52039
1.4	0.08881	2.9	0.20929	4.4	0.55715
1.5	0.09360	3.0	0.22266	4.5	0.59672

$$\text{slope } (m) = \frac{1}{137.88}\left(\frac{e^{\lambda 235 t} - 1}{e^{\lambda 238 t} - 1}\right); \lambda\,(^{238}\text{U}) = 1.55125 \times 10^{-10}\text{yr}^{-1};$$

$$\lambda\,(^{235}\text{U}) = 9.8485 \times 10^{-10}\text{yr}^{-1}$$

iterative procedure, preferably with the help of a computer, to obtain a value of t that satisfies the equation with an acceptable level of residual. Approximate solutions, however, can be obtained by preparing a table of calculated slopes (m) corresponding to selected values of t (Table 10.3) and interpolating between appropriate values of t for a particular value of the slope (see Example 10–2). A computer code called *CLEO* (Common Lead Evaluation using Octave), is also available on the web (http://www.iamg.org/CGEditor/index.htm) for calculation of regressions, using the algorithm after York (1969), and the corresponding ^{207}Pb–^{206}Pb age (Gaab *et al*., 2006).

Example 10–2: Calculation of "207–206" model age of the black shale sequence of the Niutitang Formation, China, from measured lead isotope ratios listed in Jiang et al. (2006)

A plot of ^{207}Pb/^{204}Pb versus ^{206}Pb/^{204}Pb ratios for the black shale whole-rock samples given in Jiang *et al*. (2006) defines an isochron with a slope of 0.0580 (Fig. 10.8), which corresponds to an age (t) between 0.5 Ga (^{207}Pb*/^{206}Pb* = 0.0572) and 0.6 Ga (^{207}Pb*/^{206}Pb* = 0.0599) (Table 10.3). We can calculate an approximate value of t by interpolation between these two limits, using the lever rule:

$$\frac{0.6 - 0.5}{0.0599 - 0.0572} = \frac{0.6 - t}{0.0599 - 0.0580}$$

t = 530 Ma

An iterative procedure in which the interpolation is made between successively narrower limits would yield an age of 531 Ma. Thus our time-saving approximation in this case results in an error of less than 0.2%.

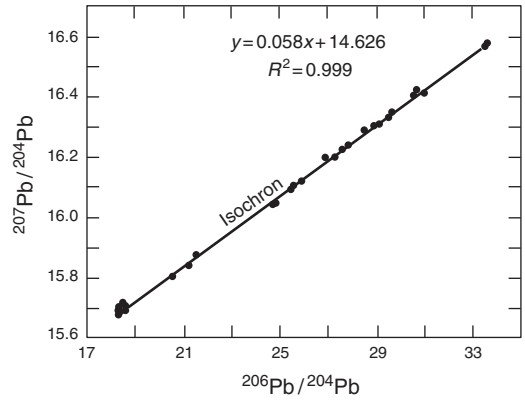

Fig. 10.8 ^{207}Pb–^{206}Pb isochron for the black shale sequence of the Niutitang Formation, China. The isotope ratios are from Jiang *et al*. (2006). The slope of the isochron is 0.0580 and the age calculated by interpolation (Table 10.3) is 530 Ma.

This dating method works better than the U–Pb and Th–Pb methods (equations 10.19, 10.20, and 10.21) because the "207–206 date" does not depend on the present-day U content of the sample and, therefore, is not affected by recent loss of U, for example, by chemical weathering.

The whole-rock lead method of dating was first applied to meteorite samples. From analysis of lead isotopes in three stony meteorites and two iron meteorites (one of which was the Canyon Diablo meteorite), Patterson (1956) was the first to calculate an age of 4.55 ± 0.05 Ga from a Pb–Pb isochron diagram (λ_{238} = 1.537 × 10^{-10} yr^{-1}; λ_{235} = 9.72 × 10^{-10} yr^{-1}). He also showed that the isotopic composition of terrestrial lead in recent oceanic sediment plots on the isochron and concluded that the age of the Earth is essentially the same as that of meteorites. [This is also corroborated by the fact the isotopic composition of Os of the Earth's mantle fits the Re–Os isochron for iron meteorites and the metallic phase of chondrites (see section 10.4.4). Subsequent studies have shown that the Pb–Pb ages of meteorites lie between 4.55 Ga and 4.57 Ga (Allègre *et al*., 1995).

Common lead method

This method is particularly useful for dating sulfide mineral deposits, which commonly contain Pb-bearing minerals. *Common lead* refers to the Pb that occurs in minerals whose U : Pb and Th : Pb ratios are so low that its isotopic composition does not change appreciably with time. The preferred common-lead mineral for lead-isotope analysis is galena (PbS), which is widely distributed in mineral deposits. When galena is not available, other base metal sulfide minerals containing trace amounts of Pb and even K-feldspar, in which Pb^{2+} replaces K^+ to a small extent, may be used.

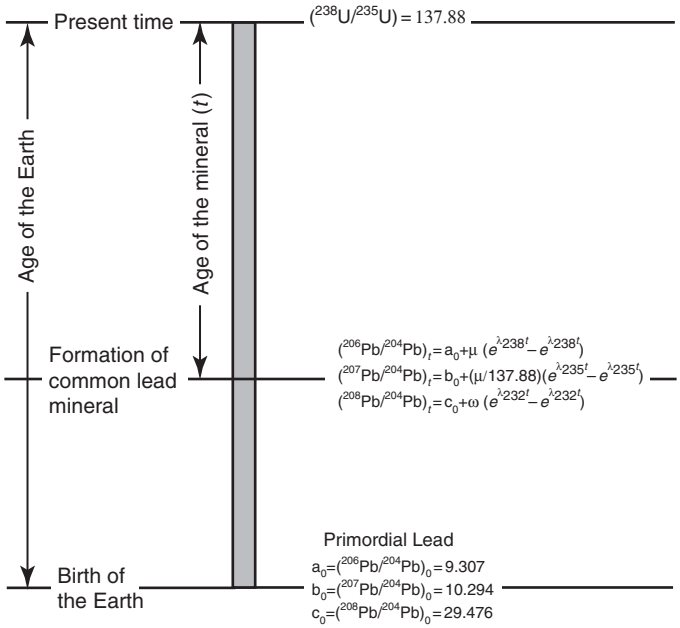

Fig. 10.9 Schematic representation of the formulation of the Holmes–Houtermans single-stage lead evolution model. The lead isotope ratios at time t are assumed to be the same as at the present time.

Single-stage leads. The simplest formulation of the lead isotope evolution is the Holmes–Houtermans single-stage model (Holmes, 1946; Houtermans, 1946), which is based on the premise that present-day isotopic ratios of common lead are the same as those at the time of its formation (Fig. 10.9). The model involves several assumptions, which are as follows (Cannon et al., 1961).

(1) The *primordial lead*, the lead at the birth of the Earth (time T = 4.55 Ga), had a unique and uniform isotopic composition, which is assumed to be the values in the troilite phase (FeS) of the Canyon Diablo meteorite because the Earth and meteorites are believed to have formed at the same time from an isotopically homogeneous solar nebula. The lead in this troilite is the least radiogenic lead ever found. It is virtually free of U and Th, and the isotopic composition of lead in this phase, therefore, can reasonably be assumed to have remained the same since its crystallization. The currently accepted values of the primordial ratios, commonly denoted as a_0, b_0, and c_0, are (Tatsumoto *et al.*, 1973):

$a_0 = (^{206}Pb/^{204}Pb) = 9.307$

$b_0 = (^{207}Pb/^{204}Pb) = 10.294$

$c_0 = (^{208}Pb/^{204}Pb) = 29.476$

(2) The changes in the $^{238}U/^{204}Pb$, $^{235}U/^{204}Pb$, and $^{232}Th/^{204}Pb$ ratios in any given region of the Earth were entirely due to radioactive decay within one or more closed systems, with U/Pb and Th/Pb ratios maintained at constant values in each system.

(3) The formation of galena (or other Pb-bearing minerals) during a mineralization event represents the separation of Pb from a mantle or crustal source; the lead-isotope ratios of the source are incorporated in the mineral without fractionation and are frozen in the mineral. In other words, the present-day lead isotopic ratios ($^{206}Pb/^{204}Pb$, $^{207}Pb/^{204}Pb$, and $^{208}Pb/^{204}Pb$) in a sample of galena are the same as they were at the time of its separation from the source.

(4) The lead source is an infinite reservoir, so that withdrawal of some Pb, U, and Th from the source by magmas, ore-forming fluids, or other mechanisms has not significantly disturbed the ratios involving the radioactive parent isotopes ^{238}U, ^{235}U, or ^{232}Th.

Commonly, the *single-stage lead evolution curve* for a system of given μ (= $^{238}U/^{204}Pb$) is constructed by plotting calculated values of $^{206}Pb/^{204}Pb$ (x axis) and $^{207}Pb/^{204}Pb$ (y axis) corresponding to a series of chosen values of t (geologic age) lying between $t = T$ (the age of the Earth) and $t = 0$ (the present time), using equations (10.30) and (10.31) (see Box 10.2)

$$\left(\frac{^{206}\text{Pb}}{^{204}\text{Pb}}\right)_t = a_0 + \mu\,(e^{\lambda 238 T} - e^{\lambda 238 t}) \qquad (10.30)$$

Box 10.2 Equations for the common lead method of geochronology

Notations

$$\frac{^{206}\text{Pb}}{^{204}\text{Pb}} = a_0 = 9.307 \quad \frac{^{207}\text{Pb}}{^{204}\text{Pb}} = b_0 = 10.294 \quad \frac{^{208}\text{Pb}}{^{204}\text{Pb}} = c_0 = 29.476$$

$$\frac{^{238}\text{U}}{^{204}\text{Pb}} = \mu \frac{^{232}\text{Th}}{^{204}\text{Pb}} = \omega \frac{^{232}\text{Th}}{^{238}\text{U}} = \kappa \left(\frac{^{238}\text{U}}{^{235}\text{U}}\right)_{\text{present}} = 137.88$$

Equations for single-stage growth curves and primary isochrons
According to the single-stage model, the $^{206}Pb/^{204}Pb$, $^{207}Pb/^{204}Pb$, and $^{208}Pb/^{204}Pb$ ratios of common lead that got separated, without isotope fractionation, from a U–Th–Pb reservoir t years ago are given by:

$$\left(\frac{^{206}\text{Pb}}{^{204}\text{Pb}}\right)_t = \left(\frac{^{206}\text{Pb}}{^{204}\text{Pb}}\right)_0 + \frac{^{238}\text{U}}{^{204}\text{Pb}}(e^{\lambda 238 T} - 1) - \frac{^{238}\text{U}}{^{204}\text{Pb}}(e^{\lambda 238 t} - 1) = a_0 + \mu\,(e^{\lambda 238 T} - e^{\lambda 238 t}) \qquad (10.30)$$

$$\left(\frac{^{207}\text{Pb}}{^{204}\text{Pb}}\right)_t = \left(\frac{^{207}\text{Pb}}{^{204}\text{Pb}}\right)_0 + \frac{^{235}\text{U}}{^{204}\text{Pb}}(e^{\lambda 235 T} - 1) - \frac{^{235}\text{U}}{^{204}\text{Pb}}(e^{\lambda 235 t} - 1) = b_0 + \frac{\mu}{137.88}\,(e^{\lambda 235 T} - e^{\lambda 235 t}) \qquad (10.31)$$

Box 10.2 (Cont'd)

$$\left(\frac{^{208}Pb}{^{204}Pb}\right)_t = \left(\frac{^{208}Pb}{^{204}Pb}\right)_0 + \frac{^{232}Th}{^{204}Pb}(e^{\lambda_{232}T} - 1) - \frac{^{232}Th}{^{204}Pb}(e^{\lambda_{232}t} - 1)$$
$$= c_0 + \mu\kappa\,(e^{\lambda_{232}T} - e^{\lambda_{232}t}) \qquad (10.32)$$

Combining equations (10.30) and (10.31), we get

$$\frac{\left(\frac{^{207}Pb}{^{204}Pb}\right)_t - b_0}{\left(\frac{^{206}Pb}{^{204}Pb}\right)_t - a_0} = \frac{1}{137.88}\left(\frac{e^{\lambda_{235}T} - e^{\lambda_{235}t}}{e^{\lambda_{238}T} - e^{\lambda_{238}t}}\right) \qquad (10.33)$$

which is the equation of a straight line in coordinates of $^{206}Pb/^{204}Pb$ (x axis) and $^{207}Pb/^{204}Pb$ (y axis), with origin at (a_0, b_0) and slope (m) given by

$$m = \frac{\left(\frac{^{207}Pb}{^{204}Pb}\right)_t - b_0}{\left(\frac{^{206}Pb}{^{204}Pb}\right)_t - a_0} = \frac{1}{137.88}\left(\frac{e^{\lambda_{235}T} - e^{\lambda_{235}t}}{e^{\lambda_{238}T} - e^{\lambda_{238}t}}\right) \qquad (10.34)$$

This straight line represents the isochron corresponding to age t. Note that the slope of the isochron is a function of t but is independent of the value of μ, whereas the isotope ratios are functions of both t and μ (equations 10.30–10.32).

Similar equations can be written relating ^{206}Pb and ^{208}Pb, and ^{207}Pb and ^{208}Pb.

$$\left(\frac{^{207}Pb}{^{204}Pb}\right)_t = b_0 + \frac{\mu}{137.88}\,(e^{\lambda_{235}T} - e^{\lambda_{235}t}) \qquad (10.31)$$

(Single-stage evolution curves can also be represented in coordinates of $^{206}Pb/^{204}Pb$ and $^{208}Pb/^{204}Pb$, or $^{207}Pb/^{204}Pb$ and $^{208}Pb/^{204}Pb$.) Each point on the single-stage curve marks the theoretical lead isotope ratios corresponding to a particular value of t when that Pb was separated from its source region and incorporated into a common lead mineral such as galena. The straight line joining such a point to the origin is the corresponding *isochron* and its slope (m) is given by

$$m = \frac{1}{137.88}\left(\frac{e^{\lambda_{235}T} - e^{\lambda_{235}t}}{e^{\lambda_{238}T} - e^{\lambda_{238}t}}\right) \qquad (10.34)$$

Note that the slope of the isochron is independent of the value of μ so that all single-stage leads that were removed from sources with different μ but at the same time t must lie on the isochron corresponding to time t. For a source region of known μ, the value of t is defined by the intersection of the corresponding growth curve with the isochron. The isochron representing leads corresponding to $t = 0$ is called the *geochron* because all modern single-stage leads in the Earth and in meteorites must lie on it. For the purpose of illustration, a set of single-stage evolution curves for reservoirs with different assumed values of μ and corresponding isochrons for a few selected values of t are shown in Fig. 10.10.

It may appear that once we have measured the lead isotopic ratios, $(^{206}Pb/^{204}Pb)_t$ and $(^{206}Pb/^{204}Pb)_t$, in a sample,we should be able to calculate t from the slope of the corresponding isochron (equation 10.34). This equation, however, is transcendental and has to be solved the same way as equation (10.29) (discussed earlier) – either by an iterative procedure or by interpolation between appropriate values of t for a particular value of the slope (Table 10.4). After the model age has been calculated, we can use equation (10.30) or (10.31) to solve for μ (see Example 10–2). The computer code *Isoplot* (version 3.00) by Ludwig (2003) can be used for constructing single-stage growth curves and isochrons, and for calculating the age corresponding to any point on the growth curve.

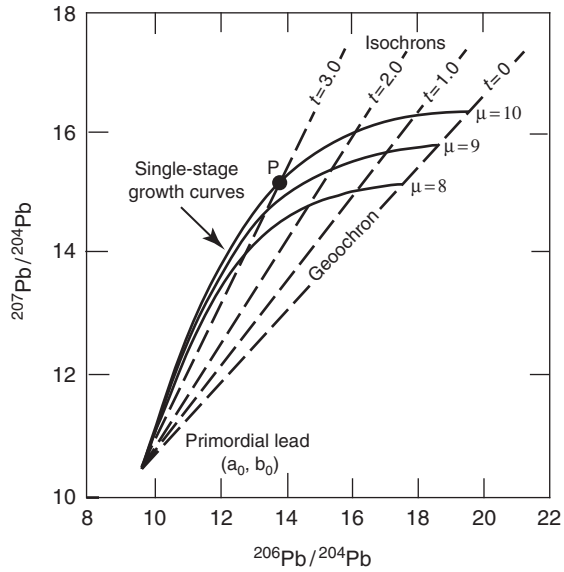

Fig. 10.10 Single-stage lead evolution curves for U–Pb systems with present-day μ (= $^{238}U/^{204}Pb$) values of 8, 9, and 10. The curves were constructed by solving equations (10.28) and (10.29) for different chosen values of t, assuming that the age of the Earth (T) = 4.55 Ga. The straight lines are isochrons for T = 4.55 Ga, and selected values of t (3.0, 2.0, 1.0, and 0 billion years); the isochron for $t = 0$ is called the geochron. The coordinates of point P represent $^{206}Pb/^{204}Pb$ and $^{207}Pb/^{204}Pb$ ratios of a galena lead that was withdrawn 3.0 Ga froma source region of $\mu = 10.0$; the model age of this galena is 3.0 Ga. $a_0 = 9.307$, $b_0 = 10.294$, $\lambda_{238} = 1.55 \times 10^{-10}\,yr^{-1}$, and $\lambda_{235} = 9.85 \times 10^{-10}\,yr^{-1}$.

Table 10.4 Calculated values of slopes (m) of isochrons for selected model ages (t), using equation (10.34)

t (Ga)	Slope (m)	t (Ga)	Slope (m)	t (Ga)	Slope (m)	t (Ga)	Slope (m)
0.2	0.6356	1.4	0.7815	2.6	1.0341	3.8	1.5039
0.4	0.6551	1.6	0.8142	2.8	1.0930	4.0	1.6175
0.6	0.6763	1.8	0.8501	3.0	1.1583	4.2	1.7450
0.8	0.6992	2.0	0.8895	3.2	1.2310	4.4	1.8885
1.0	0.7243	2.2	0.9330	3.4	1.3121	4.5	1.9670
1.2	0.7516	2.4	0.9810	3.6	1.0341		

$m = (1/137.88)\,(e^{\lambda 235T} - e^{\lambda 235t}) / (e^{\lambda 238T} - e^{\lambda 238t})$

$\lambda\,(^{238}U) = 1.55125 \times 10^{-10}\,yr^{-1}$; $\lambda\,(^{235}U) = 9.8485 \times 10^{-10}\,yr^{-1}$; $T = 4.55 \times 10^{9}\,yr$

Example 10–2: Calculation of the age (t) of a galena sample from its lead isotope composition, assuming that the lead evolution conformed to the Holmes–Houtermans model. Use values of a_0, b_0, λ_{238}, λ_{235}, and T as given in the text

Suppose, the lead isotope ratios of a single-stage galena from a zinc–lead sulfide ore deposit are: $^{206}Pb/^{204}Pb = 14.1855$, and $^{207}Pb/^{204}Pb = 15.3899$. What is the age ($t$) of this galena?

To determine the Holmes–Houtermans model age of this galena sample, we first calculate the slope of the isochron corresponding to age t from the given values of the isotope ratios (equation 10.34):

$$m = \frac{\left(\frac{^{207}Pb}{^{204}Pb}\right)_t - b_0}{\left(\frac{^{206}Pb}{^{204}Pb}\right)_t - a_0} = \frac{15.3899 - 10.294}{14.1855 - 9.307} = \frac{5.0959}{4.8785} = 1.0446$$

This value of slope corresponds to an age (t) lying between 2.6 Ga (slope = 1.0341) and 2.8 Ga (slope = 1.0930) (Table 10.4). We now calculate the value of t by applying the lever rule:

$$t = 2.6 + \frac{(2.8 - 2.6)\,(1.0446 - 1.0341)}{1.0930 - 1.0341} = 2.6 + 0.0356$$
$$= 2.636\ \text{Ga}$$

The error resulting from this approximation is very small – theoretical calculation, as for Table 10.4, would yield a slope of 1.0446 for $t = 2.637$ Ga.

We can also calculate the $^{238}U/^{204}Pb$ ratio (or μ) of the source region of lead for this galena by using equation (10.30):

$$\mu = \frac{\frac{^{206}Pb}{^{204}Pb} - a_0}{e^{\lambda 238T} - e^{\lambda 238t}} = \frac{14.1855 - 9.307}{e^{(1.5513 \times 10^{-10})\,(4.55 \times 10^{9})} - e^{(1.5513 \times 10^{-10})\,(2.636 \times 10^{9})}}$$
$$= \frac{4.8785}{e^{0.7058} - e^{0.4089}} = \frac{4.8785}{2.0255 - 0.5203} = \frac{4.8785}{0.5203} = 9.38$$

Anomalous leads. If the isotopic composition of the lead contained in a rock or a mineral deposit can be accounted for by the single-stage evolution model (i.e., the composition plots on the single-stage evolution curve), it is called *single-stage lead* or *ordinary lead*, and its model age gives the time of its formation within experimental error; if not, it is called *anomalous lead*, and its model age may be appreciably different from its actual time of formation. An unmistakable example of anomalous lead is the J-type lead (Russell and Farquhar, 1960), so named after its type occurrence in the galena–sphalerite ores of Joplin (Missouri, USA), which contains excess radiogenic lead and yields model ages that are younger than the age of the ore deposit inferred from other lines of evidence.

Many leads are anomalous in the context of the Holmes–Houtermans model, because their lead isotope ratios have been evaluated with reference to an evolution model that assumes that the μ and ω values of the lead reservoir have changed with time only by radioactive decay and not by other processes such as differentiation and homogenization. Such an assumption is unrealistic in view of the dynamic evolution of the Earth involving repeated interaction between the mantle and the crust. This realization has led to several recently proposed lead evolution models that allow for variation in μ and ω values of the lead reservoir by mixing of leads of different isotopic compositions. For example, Stacey and Kramers (1975) constructed an "average" lead growth curve incorporating a two-stage process that involved a change in the μ and ω values of the reservoir (by geochemical differentiation) at 3.7 Ga and found this to yield good model ages for lead samples of different ages (Fig. 10.11). Their model postulates a first stage of lead evolution from a primordial composition assumed to be that of meteoritic troilite lead ($\mu = 7.19$, $\omega = 32.19$) beginning at 4.57 Ga, and a second stage evolution beginning at 3.7 Ga with ($\mu \approx 9.74$, $\omega \approx 37.19$) in those portions of the Earth that took part in the mixing events, giving rise to "average" lead. Doe and Zartman (1979) discussed the lead isotope data from several geologic environments in relation to four growth curves generated by a dynamic lead evolution model:

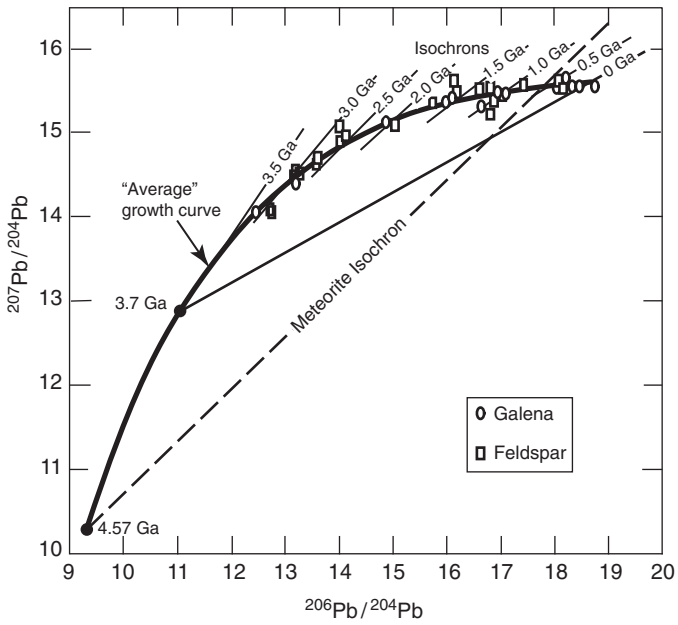

Fig. 10.11 Lead isotopic ratios of 13 galena samples from conformable deposits and 23 least radiogenic feldspar leads in relation to the two-stage lead evolution curve of Stacey and Krammers (1975). For the first-stage evolution $\mu = 7.19$ and for the second stage $\mu = 9.74$; the first stage began at $t = T$ (4.5 Ga), and the second stage at $t = 3.7$ Ga. The difference between the accepted age and the model age obtained from the two-stage lead evolution curve lie within ± 100 Ma for all galena samples (actually within ±50 Ma for all except the two youngest samples) and for 17 out of 23 feldspar samples. (After Stacey and Kramers 1975.)

(i) a curve for the mantle lead ($\mu = 8.92$), (ii) a curve for the "orogene," representing a balance of lead input from the mantle, upper crust, and lower crust sources ($\mu = 10.87$), corresponding to the "average" curve of Stacey and Kramers (1975); (iii) a curve reflecting lead contribution from only the upper crust to the orogene ($\mu = 12.24$); and (iv) a curve reflecting lead contribution from the lower crust only to the orogene ($\mu = 5.89$). When combined with regional and local geologic data, such dynamic models offer significant improvements in the interpretation of anomalous leads, although they often do not lead to unequivocal identification of the lead source.

10.3.4 Rhenium–osmium system

Osmium, a platinum-group element (PGE), has seven naturally occurring isotopes – $^{184}_{76}$Os (0.023%), $^{186}_{76}$Os (1.600%), $^{187}_{76}$Os (1.510%), $^{188}_{76}$Os (13.286%), $^{189}_{76}$Os (16.251%), $^{190}_{76}$Os (26.369%), and $^{192}_{76}$Os (40.957%) – all of which are stable. Rhenium has two naturally occurring isotopes – stable $^{185}_{75}$Re (37.398%) and radioactive $^{187}_{75}$Re (62.602%). The basis of age dating by Re–Os isotopes is the *b*-decay of $^{187}_{75}$Re to $^{187}_{76}$Os ($^{187}_{75}\text{Re} \Rightarrow {}^{187}_{76}\text{Os} + \beta^- + \bar{\nu}$ + energy).

For the decay of $^{187}_{75}$Re to $^{187}_{76}$Os, the geochronologic equation incorporating the nonradiogenic isotope $^{186}_{76}$Os for normalization takes the form

$$\frac{^{187}\text{Os}}{^{186}\text{Os}} = \left(\frac{^{187}\text{Os}}{^{186}\text{Os}}\right)_0 + \frac{^{187}\text{Re}}{^{186}\text{Os}}\,(e^{\lambda_{\text{Re}}t} - 1) \qquad (10.35)$$

where $(^{187}\text{Os}/^{186}\text{Os})_0$ is the initial ratio, $^{187}\text{Os}/^{186}\text{Os}$ and $^{187}\text{Re}/^{186}\text{Os}$ are the present-day ratios, λ_{Re} is the decay constant of ^{187}Re, and t is the geologic age of the sample. There is some uncertainty about the value of λ_{Re}. As discussed by Dickin (1995), the most appropriate value for use in geologic age studies is $1.64 \times 10^{-11}\,\text{yr}^{-1}$ (half-life $= 42.3 \times 10^9$ yr) determined by Lindner *et al.* (1989). Equation (10.35) is analogous to equation (10.15) and the procedure for age determination is the same as described for the Rb–Sr method.

The Re–Os method is particularly attractive for dating mineral deposits containing phases, such as molybdenite (MoS_2) or copper sulfides, that generally carry high Re : Os ratios, although the possible mobility of Re in hypogene and near-surface environments (Walker *et al.*, 1989; McCandless *et al.*, 1993) is a potential problem. A problem in using Os-rich minerals of the platinum-group elements, such as osmiridium (OsIr) and laurite [Ru(Os,Ir)S_2], for geochronology is that a significant fraction of ^{186}Os in the sample could have been generated by the rare long-lived unstable isotope ^{190}Pt, as in copper ores of the Sudbury igneous complex (Walker *et al.*, 1991).

The Os-rich minerals, however, are very useful for tracing how the mantle osmium isotopic composition has evolved as a function of time from its primordial value of 0.807 ± 0.006 (Fig. 10.12a). The consistent association of these minerals with ultramafic rocks derived from mantle sources suggests that the minerals inherited the mantle Os isotopic composition at the time of their formation, and this composition has not changed with time because these minerals incorporated virtually no Re. As shown in Fig. 10.12b, a plot of $^{187}\text{Os}/^{186}\text{Os}$ ratios of a suite of these minerals (excluding the laurite sample from the Bushveld Complex) against time define a highly correlated straight line, suggesting that the mantle evolved with a homogeneous Re : Os ratio (despite the formation of the crust by magmatic activity within it) that changed only as a result of ^{187}Re decay. The regression equation for the Os-evolution line is:

$$^{187}\text{Os}/^{186}\text{Os} = 1.040 - 0.050768\,t \qquad (10.36)$$

where t is the geological age of the sample (i.e., the time that has elapsed since the removal of the Os-mineral from its source in the mantle) in units of Ga. This equation can be used as a geochronometer to date common Os minerals (i.e., Os minerals that formed practically without incorporating any Re) if they had formed from a mantle source whose Os isotopic composition was the same as predicted by the Os-evolution line in Fig 10.12b, and which evolved in a system closed to Os and Re. Application of this simple technique, which equires the measurement only of

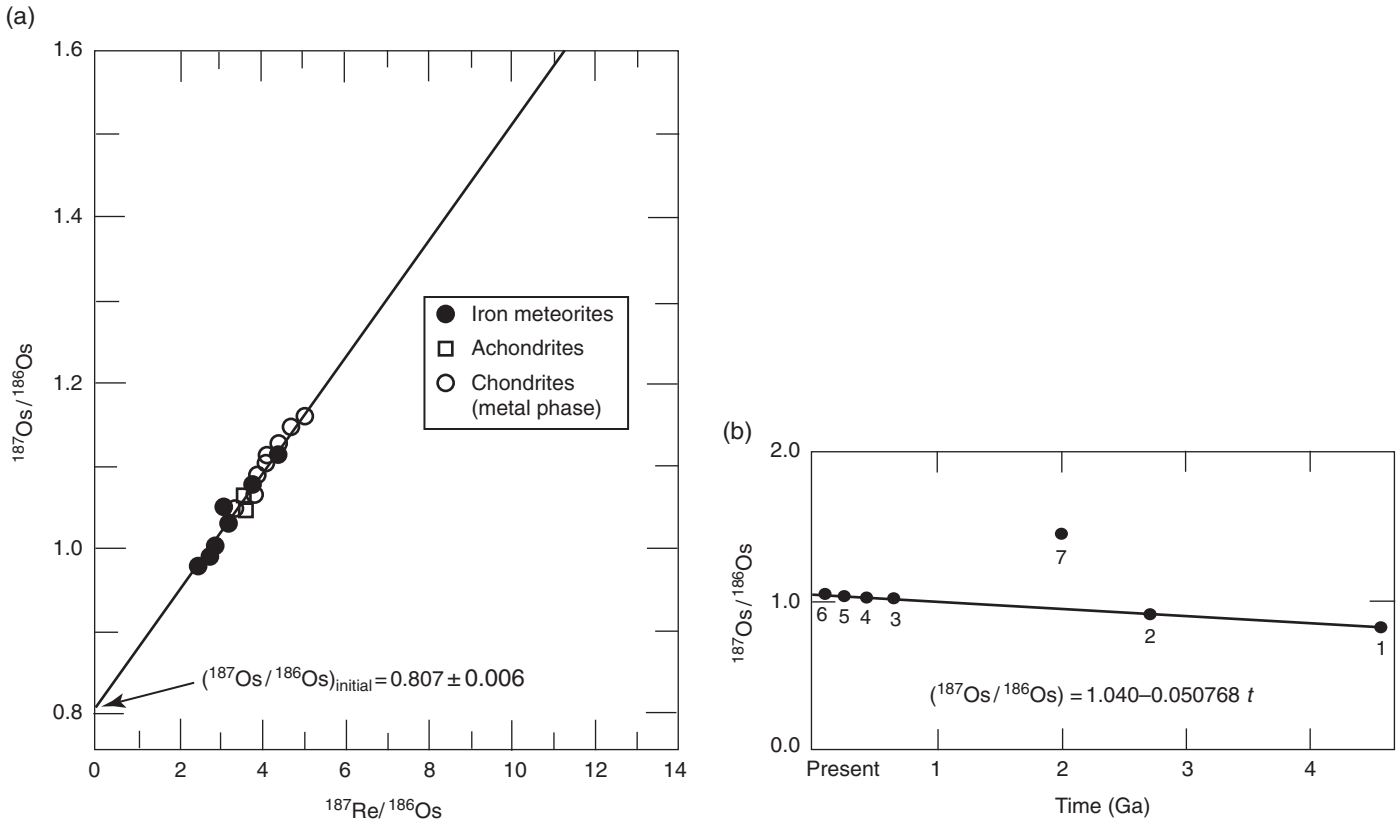

Fig. 10.12 (a) Re–Os isochron for iron meteorites and metallic phases in chondrites. The colinearity of the data indicates that the meteorites formed within a narrow time range from a primordial source that was isotopically homogeneous with respect to Os. The primitive mantle composition included in this figure, $^{187}Re/^{186}Os = 3.34$, and the present $^{187}Os/^{186}Os = 1.040$ are taken from the mantle evolution curve plotted in Fig. 10.12b. The fit of the estimated mantle composition (Luck and Allègre, 1983) to the Re–Os isochron is evidence that the parent bodies of meteorites and the Earth formed at about the same time from the same primordial source. (Sources of data: Allègre and Luck, 1980; Luck and Allègre, 1983.) (b) Evolution of the isotopic composition of osmium in the Earth's mantle based on samples of iron meteorites, osmiridium, and laurit. Data points for the Bushveld Complex (McCandless and Ruiz, 1991) plot above the mantle evolution curve, and probably reflect crustal contamination.

$^{187}Os/^{186}Os$ ratios in samples, is limited by the rarity of Os-rich minerals. Attempts to apply the technique to date Ni–Cu sulfides (e.g., Luck and Allègre, 1984) were not successful, probably because of open-system behavior of the sulfides.

10.3.5 Potassium (^{40}K)–argon (^{40}Ar) method

The radioactive isotope $^{40}_{19}K$, which constitutes only a minute fraction of naturally occurring potassium (effectively a constant value of 0.01167 atom % in all rocks and minerals), undergoes branched decay to $^{40}_{20}Ca$ by β^- emission (88.8% of the ^{40}K nuclides) and to $^{40}_{18}Ar$ by electron capture and β^+ decay (11.2% of the ^{40}K nuclides). The radiogenic ^{40}Ca and ^{40}Ar generated over time t in a K-bearing system closed to K, Ca, and Ar can be expressed as

$$^{40}Ca^* + {}^{40}Ar^* = {}^{40}K(e^{\lambda_K t} - 1) \tag{10.37}$$

where ^{40}Ca and ^{40}Ar represent the daughters generated over time t, and λ_K is the total decay constant of ^{40}K. Denoting the decay constants of the branched decay of ^{40}K to ^{40}Ca and to ^{40}Ar as λ_β and λ_{ec}, respectively, and using the recommended values of the decay constants given in Steiger and Jäger (1977),

$$\begin{aligned}\lambda_K = \lambda_\beta + \lambda_{ec} &= (4.962 \times 10^{-10}\,yr^{-1}) + (0.581 \times 10^{-10}\,yr^{-1}) \\ &= 5.543 \times 10^{-10}\,yr^{-1}\end{aligned} \tag{10.38}$$

The branched decay of ^{40}K results in two potential geochronometers. The decay to ^{40}Ca has been used, for example, by Marshall and DePaolo (1982) to date the Pikes Peak batholith of Colorado, but the method has limited application as a dating tool because in most rock systems the radiogenic ^{40}Ca is overwhelmed by the abundance of nonradiogenic ^{40}Ca, the latter constituting about 97% of the total Ca in terrestrial samples. The decay to ^{40}Ar, on the other hand, has been widely used to date K-bearing minerals, volcanic glass, and whole rocks. Minerals suitable for K–Ar dating include feldspars, feldspathoids, micas, amphiboles, and pyroxenes.

In general, the total number of ^{40}Ar atoms in a rock or mineral sample is the sum of three components:

$$^{40}Ar = (^{40}Ar)_0 + {}^{40}Ar^* = (^{40}Ar)_{atm} + (^{40}Ar)_{excess} + {}^{40}Ar^* \quad (10.39)$$

where $^{40}Ar^*$ is the radiogenic Ar produced by decay of ^{40}K in the sample subsequent to its crystallization or since it became a closed system, and $(^{40}Ar)_0$ is the total amount of initial Ar atoms in the sample. The latter is composed of $(^{40}Ar)_{atm}$, the atmospheric Ar adsorbed onto or contained within the sample, and $(^{40}Ar)_{excess}$, the *excess argon* that was derived by outgassing of old rocks in the crust and mantle and retained by the sample at the time of its formation.

The fraction of ^{40}K atoms that decay into $^{40}Ar^*$ is $(\lambda_{ec}/\lambda_K)^{40}K$, so that the geochronologic equation for the total amount of ^{40}Ar atoms in a closed K-bearing system can be written as

$$\boxed{^{40}Ar = (^{40}Ar)_0 + {}^{40}Ar^* = (^{40}Ar)_0 + \frac{\lambda_{ec}}{\lambda_K}\ {}^{40}K\ (e^{\lambda_K t} - 1)} \quad (10.40)$$

where t is the geologic age of the sample. As it is very difficult to determine $(^{40}Ar)_0$ in a sample and a mineral is unlikely to trap appreciable amounts of the inert argon gas in the crystal structure at the time of its formation, in the conventional ^{40}K–^{40}Ar method it is assumed that the sample contained no initial argon, that is, $(^{40}Ar)_0 = 0$. The assumption does not introduce significant error in the case of samples highly enriched in $^{40}Ar^*$ relative to $(^{40}Ar)_0$. Equation (10.40), then, simplifies to

$$^{40}Ar\ = {}^{40}Ar^* = \frac{\lambda_{ec}}{\lambda_K}\ {}^{40}K(e^{\lambda_K t} - 1) \quad (10.41)$$

which can be solved for t if the concentrations of ^{40}K and $^{40}Ar^*$ in the sample are known from measurements:

$$t = \frac{1}{\lambda_K} \ln \left[\frac{^{40}Ar^*}{^{40}K} \left(\frac{\lambda_K}{\lambda_{ec}} + 1 \right) \right] \quad (10.42)$$

In the conventional ^{40}K–^{40}Ar method, ^{40}K and ^{40}Ar contents are measured on separate aliquots of the sample to be dated. In practice, the total K content is measured on one aliquot by some standard analytical technique (such as X-ray fluorescence, atomic absorption, or flame photometry); the ^{40}K content is obtained by multiplying the total concentration of K in the sample by a factor of 0.0001167, the fractional abundance of ^{40}K. The other aliquot is heated to fusion within an ultrahigh vacuum system (to minimize argon contamination from the atmosphere), and the released gas is analyzed in a mass spectrometer, using known quantities of ^{38}Ar as a tracer. The amount of $^{40}Ar^*$ in the sample is calculated by subtracting the nonradiogenic ^{40}Ar liberated during the experiment from the measured value of ^{40}Ar. The nonradiogenic ^{40}Ar is assumed to be atmospheric contamination and to have the same $^{40}Ar/^{36}Ar$ ratio (= 295.5) as the present atmosphere (Dalrymple and Lanphere, 1969). Thus, the correction is made by measuring the ^{36}Ar content of the argon gas released during the experiment, and multiplying it by 295.5 to get the amount of contaminating ^{40}Ar:

$$^{40}Ar^* = {}^{40}Ar_m - {}^{36}Ar_m(295.5) \quad (10.43)$$

where the subscript "m" means the value measured by the mass spectrometer.

The assumption of no initial argon in a sample is a limitation of the conventional K–Ar dating method described above; it tends to overestimate the age of a sample because of the presence of a small amount of nonradiogenic Ar component (in the order of $10^{-9}\,cm^3\,g^{-1}$; Roddick, 1978) within minerals at the time of their crystallization. However, for a group of K-bearing minerals of the same age and identical $(^{40}Ar)_0$, a condition likely to be satisfied if the analysis is restricted to several K-bearing minerals coexisting in the same rock specimen, the age and initial ratio can be determined by the isochron method similar to that discussed earlier for the Rb–Sr and Sm–Nd systems. The equation for the ^{40}K–^{40}Ar isochron method, normalized to the abundance of the nonradiogenic isotope ^{36}Ar, is

$$\boxed{\frac{^{40}Ar}{^{36}Ar} = \left(\frac{^{40}Ar}{^{36}Ar} \right)_0 + \frac{\lambda_{ec}}{\lambda_K} \frac{^{40}K}{^{36}Ar} (e^{\lambda_K t} - 1)} \quad (10.44)$$

The age t can be calculated from the slope (m) of the isochron, a straight line, defined in $^{40}Ar/^{36}Ar$ (y axis) – $^{40}K/^{36}Ar$ (x axis) space by the relation

$$m = \left(\frac{\lambda_{ec}}{\lambda_K} \right) (e^{\lambda_K t} - 1) \quad (10.45)$$

Equation (10.45) can be rearranged to obtain the following expression for t:

$$t = [\ln (m\ \frac{\lambda_K}{\lambda_{ec}} + 1)]/\lambda_K \quad (10.46)$$

The y-axis intercept of the isochron gives the value of $(^{40}Ar/^{36}Ar)_0$, which represents the sum of the atmospheric component and the excess argon retained by the samples at the time of their formation:

$$\left(\frac{^{40}Ar}{^{36}Ar} \right)_0 = \left(\frac{^{40}Ar}{^{36}Ar} \right)_{atm} + \left(\frac{^{40}Ar}{^{36}Ar} \right)_{excess} = 295.5 + \left(\frac{^{40}Ar}{^{36}Ar} \right)_{excess} \quad (10.47)$$

This formulation assumes that all the samples have the same nonradiogenic argon isotope composition, i.e., the same value of $(^{40}Ar/^{36}Ar)_0$.

The ^{40}K–^{40}Ar method is the only major dating method that involves a gaseous daughter product. Argon tends to diffuse out of many minerals to some extent, even at modest temperatures of a few hundred degrees; in such situations, the determined ^{40}K–^{40}Ar age would be erroneously younger.

In reality, a ^{40}K–^{40}Ar date calculated using equation (10.41) represents not the age but rather the time elapsed since the mineral being dated cooled through its *blocking* (or *closure*) *temperature*, the temperature below which Ar loss from a particular mineral by diffusion becomes negligible compared with its rate of accumulation. The blocking temperature of a mineral depends on the cooling rate. For example, sanidine from volcanic rocks is highly retentive because of rapid cooling, but K-feldspar from plutonic rocks is not because of slow cooling. An additional issue for the isochron method (equation 10.44) is that the blocking temperature also depends on the crystal structure and, therefore, varies from mineral to mineral. Among the common minerals in igneous and metamorphic rocks, hornblende, muscovite, and biotite retain Ar fairly well. However, if the temperature during an episode of metamorphism is maintained at a sufficiently high temperature for all the Ar to escape from a rock, the K–Ar system will be reset and the ^{40}K–^{40}Ar date will record the age of metamorphism rather than the age of mineral formation.

10.3.6 Argon (^{40}Ar)–argon (^{39}Ar) method

A useful variant of the ^{40}K–^{40}Ar method is the ^{40}Ar–^{39}Ar technique that is based on the conversion of a known fraction of the $^{39}_{19}K$ in a K-bearing sample to $^{39}_{18}Ar$ by irradiation with fast neutrons in a nuclear reactor. The efficiency of irradiation to produce ^{39}Ar is determined by irradiating a standard of known ^{39}K concentration and age (commonly referred to as the flux monitor) simultaneously with the unknown sample. The sample is heated under ultrahigh vacuum (as in the case of the conventional K–Ar approach) after irradiation, and the released gas is analyzed by mass spectrometry to obtain the $^{40}Ar^*/^{39}Ar$ ratio and to calculate the age of the sample. The calculation includes appropriate corrections for argon isotopes introduced from the atmosphere and produced within the sample by undesirable neutron reactions with calcium and potassium (Dalrymple and Lanphere, 1971, 1974; Hanes, 1991).

Since the ^{39}Ar produced is proportional to the ^{39}K content of the sample, and the ratio of ^{39}K to ^{40}K is a constant of known value, a measure of ^{39}Ar in the sample yields a measure of the ^{40}K in the same sample. Thus, the $^{40}Ar^*/^{39}$ Arratio is proportional to the $^{40}Ar^*/^{40}K$ ratio, and hence the age of the sample. The relevant age equation in this case turns out to be

$$t = \frac{1}{\lambda_K} \ln \left(\frac{^{40}Ar^*}{^{39}Ar} J + 1 \right) \tag{10.48}$$

where J, a measure of the efficiency of conversion of ^{39}K to ^{39}Ar, is given by

$$J = \frac{e^{\lambda_K t_s} - 1}{(^{40}Ar^*/^{39}Ar)_s} \tag{10.49}$$

In equation (10.49), t_s is the known age of the standard and $(^{40}Ar^*/^{39}Ar)_s$ the measured value of this ratio in the standard. An advantage of the $^{40}Ar^*/^{39}Ar$ method is that we measure a ratio of argon isotopes, which is inherently more precise than the measurement of absolute abundances of K and Ar.

The $^{40}K-^{39}Ar$ method has two variations: the *total fusion technique*, in which the sample is heated to complete fusion after irradiation, and the age is calculated from the $^{40}Ar^*/^{39}Ar$ ratio of all of the Ar released in a single experiment; and the *incremental heating* or *age spectrum* technique in which the sample is heated in incremental steps (starting at a few hundred degrees centigrade and finishing with fusion of the sample) and an apparent age is calculated from the $^{40}Ar^*/^{39}Ar$ ratio of the released argon gas corresponding to each step. This latter variation is useful in special cases, for example, where some Ar has been lost in a post-crystallization thermal event (Dalrymple and Lanphere, 1971). Because the ^{39}Ar in the sample is due to atom-per-atom conversion of ^{40}K, it is possible to liberate argon in stages from different domains of the sample and still recover full age information from each step (Dickin, 1995). If the sample has been closed to K and Ar* since the time of initial cooling, the ratio of $^{40}Ar^*$ to reactor-produced ^{39}Ar will be the same for each increment of gas released and each heating step will give the same apparent ^{40}Ar–^{39}Ar age. The result will be an age spectrum that will plot essentially as a horizontal line (or a "plateau") in a plot of apparent ^{40}Ar–^{39}Ar ages against the fraction of ^{39}Ar released, from which a meaningful age can be extracted (Fig. 10.13a). On the other hand, if Ar* was lost from only some crystallographic sites but not others, then the apparent age calculated for each heating step will be different and the age spectrum will take a more complicated form. The age of such a sample and perhaps some of its geologic history might still be inferred from the release pattern, even though its conventional $^{40}K-^{40}Ar$ age would be erroneous.

The incremental heating data can also be used to construct a $^{40}Ar/^{36}Ar$ versus $^{39}Ar/^{36}Ar$ isochron diagram (Fig. 10.13b), similar to those discussed earlier for other isotope systems. The relevant equation is

$$\left(\frac{^{40}Ar}{^{36}Ar}\right)_m = \left(\frac{^{40}Ar}{^{36}Ar}\right)_0 + \left(\frac{^{40}Ar^*}{^{39}Ar}\right)_k \left(\frac{^{39}Ar}{^{36}Ar}\right)_m \tag{10.50}$$

where the subscripts "m" and "k" refer, respectively, to measured ratios and to argon produced by potassium in the sample. Equation (10.50) defines a straight line (an isochron) in coordinates of $(^{40}Ar/^{36}Ar)_m$ and $(^{39}Ar/^{36}Ar)_m$ whose slope is the

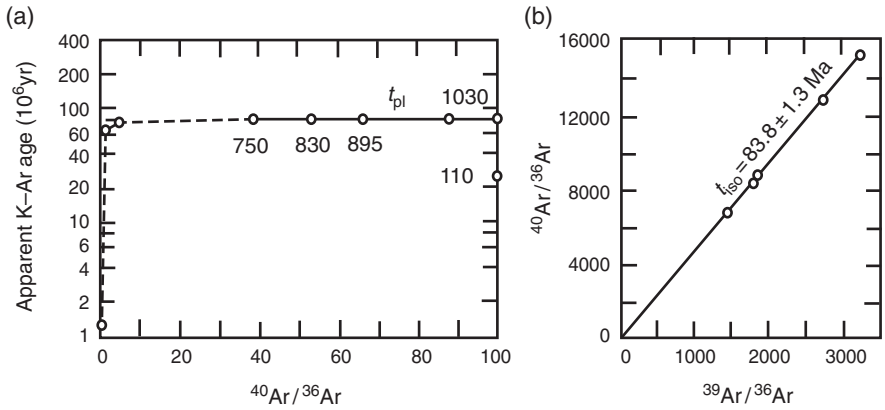

Fig. 10.13 Age of a relatively "undisturbed" muscovite sample by the ^{40}Ar–^{39}Ar method: (a) $^{40}Ar/^{39}Ar$ age spectrum diagram and (b) isochron diagram. The weighted average plateau age (t_{pl}) and the isochron age (t_{iso}) are not significantly different from each other or from the age determined by the conventional ^{40}K–^{40}Ar method (80.6 ± 1.0 Ma) at the 95% confidence level). The number by the side of each data point marks the temperature (in degrees Celsius) of the heating step, and the steps included in the calculation of the plateau age are connected by solid lines. The first three heating steps yield low apparent ages, which may indicate a small (1% or less) loss of radiogenic argon, but the error in age is indistinguishable from statistical uncertainty. On the isochron diagram, the intercept representing $(^{40}Ar/^{39}Ar)_0$ is 50 ± 128 Ma for the muscovite sample. (After Dalrymple and Lanphere, 1974.)

$^{40}Ar^*/^{39}Ar$ ratio that is related to the age of the sample by equation (10.48) and whose intercept is the initial $^{40}Ar/^{36}Ar$ ratio.

10.3.7 Carbon-14 method

Cosmogenic radionuclides are produced by the collision of cosmic rays, which contain high-energy protons and other particles, with nuclei of atoms in the atmosphere and on the Earth's surface. Table 10.5 presents a list of cosmogenic radionuclides that are important for geologic applications. In this chapter we will briefly discuss only the use of carbon-14 isotope for dating samples containing biogenic carbon; for a more detailed discussion of radiocarbon geochronology, the reader is referred to Trumbore (2000). The radiocarbon dating technique was introduced by Willard F. Libby (1908–1980) and his colleagues at the University of Chicago in 1949, an achievent that brought Libby the 1960 Nobel Prize for chemistry.

Carbon has two stable isotopes, $^{12}_{6}C$ (98.89 atom %) and $^{13}_{6}C$ (1.11 atom %), and a radioactive isotope, $^{14}_{6}C$, produced in the upper atmosphere by the interaction between cosmic-ray neutrons and the nucleus of stable $^{14}_{7}N$ atoms:

$$\text{neutron} + {}^{14}_{7}N \Rightarrow {}^{14}_{6}C + \text{proton} \qquad (10.51)$$

Most of ^{14}C is quickly oxidized to CO_2 or incorporated into CO and CO_2 molecules through exchange reactions with ^{12}C

Table 10.5 Some cosmogenic radionuclides and their applications

Parent/stable daughter	Half – life (yr)	λ (yr^{-1})	Principal applications
$^{10}_{4}Be$ / $^{10}_{5}Be$	1.5×10^6	0.462×10^{-6}	Dating marine sediment, Mn-nodules, glacial ice, quartz in rock exposures, terrestrial age of meteorites, and petrogenesis of island-arc volcanics
$^{14}_{6}C$ / $^{14}_{7}N$	5730 ± 40	0.1209×10^{-3}	Dating of biogenic carbon, calcium carbonate, terrestrial age of meteorites; carbon cycling among the Earth's carbon reservoirs
$^{26}_{13}Al$ / $^{26}_{12}Mg$	0.716×10^6	0.968×10^{-6}	Dating marine sediment, Mn-nodules, glacial ice, quartz in rock exposures, terrestrial age of meteorites
$^{32}_{14}Si$ / $^{32}_{16}Si$	276 ± 32	0.251×10^{-2}	Dating biogenic silica, glacial ice
$^{36}_{17}Cl$/ $^{36}_{16}S$, $^{36}_{18}Ar$	0.308×10^6	2.25×10^{-6}	Dating glacial ice, exposures of volcanic rocks, groundwater, terrestrial age of meteorites
$^{39}_{18}Ar$ / $^{39}_{19}K$	269	0.257×10^{-2}	Dating glacial ice, groundwater
$^{53}_{25}Mn$ / $^{53}_{24}Cr$	3.7×10^6	0.187×10^{-6}	Terrestrial age of meteorites, abundance of extraterrestrial dust in ice and sediment
$^{81}_{36}Kr$ / $^{81}_{35}Br$	0.213×10^6	3.25×10^{-6}	Dating glacial ice, cosmic-ray exposure age of meteorites
$^{182}_{72}Hf$ / $^{182}_{74}W$	9.0×10^6	7.7×10^{-8}	Dating of the formation of planetesimals and planets, and the initiation and duration of core formation in terrestrial planets

Sources of data: Faure (1986), Halliday and Lee (1999)

and ^{13}C, and dispersed rapidly through the atmosphere and the hydrosphere. The radioactive $^{14}_{6}C$ isotope decays to stable $^{14}_{7}N$ by emission of β^- particles (decay constant $\lambda_{C-14} = 1.209 \times 10^{-4}\,yr^{-1}$; half-life = 5730 ± 40 yr). A balance between the rates of production and decay of ^{14}C is responsible for maintaining a steady equilibrium concentration of ^{14}C in the atmosphere.

Plants acquire ^{14}C through consumption of $^{14}CO_2$ molecules during photosynthesis, and by absorption through the roots; animals acquire ^{14}C by eating plant material and by absorbing CO_2 from the atmosphere and the hydrosphere. As a result of rapid cycling of carbon between the atmosphere and living biosphere, the concentration (more correctly, the activity) of ^{14}C in living organisms is maintained at a constant level, which is approximately equal to that of the atmosphere (once the $^{14}C/^{12}C$ ratio has been corrected for mass-dependent isotope fractionation effects). When an organism dies it no longer absorbs $^{14}CO_2$ from the atmosphere, and the concentration of ^{14}C in the organism decreases as a function of time because of radioactive decay. Thus, the present concentration of ^{14}C in dead plant or animal material is a measure of the time elapsed since its death and is the principle underlying the carbon-14 method of dating. For the radiocarbon age of an organic matter sample to correspond with is actual age, the ratio of carbon isotopes in the measured material must not have changed – except by the radioactive decay of ^{14}C – since the death of the organism.

Radioactive decay of ^{14}C is a first-order reaction and its integrated rate equation for a sample of carbon extracted from plant or animal tissue that died t years ago is given by (see section 9.1.3; Fig. 9.2):

$$\boxed{[A]_t = [A]_0\ e^{-\lambda_{C-14}t}} \qquad (10.52)$$

where $[A]_t$ is the concentration of ^{14}C in a sample in equilibrium with the atmosphere, and $[A]_0$ is the concentration of ^{14}C in the same sample at the time of death of the animal or plant (commonly referred to as *specific activity* of ^{14}C), both measured in units of disintegrations per minute per gram of carbon (dpm $g^{-1}$of C), and λ_{C-14} is the dissociation constant for ^{14}C decay. Note that, unlike other radiometric dating methods, the ^{14}C method does not require the ratio of parent to daughter, or even the concentration of ^{14}N, in the sample. Using $\lambda_{C-14} = 1.209 \times 10^{-4}\,yr^{-1}$ and converting natural logarithm to the base 10, we obtain the following expression for t, the ^{14}C age of the sample:

$$\boxed{t\ (\text{years}) = \frac{1}{\lambda_{C-14}} \ln \frac{[A]_0}{[A]_t} = 19.035 \times 10^3\ \log \frac{[A]_0}{[A]_t}} \qquad (10.53)$$

To determine $[A]_t$ in a sample, it is first converted into CO_2 or another carbon compound, and then the concentration of ^{14}C is measured by counting the disintegrations with an ionization chamber or a scintillation counter. The value of $[A]_0$ is assumed to be known and to have been constant during the past 70,000 years, regardless of the species of plant or animal whose dead tissues are being dated and their geographic location. The best estimate of $[A]_0$ is 13.56 ± 0.07 dpm g^{-1} of C (Libby, 1955), but the value should be corrected for systematic variation of the ^{14}C content of the atmosphere in the past (Taylor, 1987; Faure, 1998).

Materials commonly used for ^{14}C dating include wood, charcoal, peat, nuts, seeds, grass, and paper. The rapid decay of ^{14}C limits the useful range of the method to about 12 half-lives or about 70,000 years (more realistically, 50,000 to 60,000 years) and, thus, its application in geology, such as dating volcanic ash and glacial events, but it is very useful for dating archeological samples, groundwater, and organic samples relevant to environmental geochemistry. A problem with dating groundwater is that it may contain carbon from dissolution of carbonates; this carbon does not contain any ^{14}C and, therefore, the groundwater may appear much older than it really is. Samples younger than about 1860 cannot be dated by the ^{14}C method owing to profound changes in the ^{14}C content of the atmosphere since the industrial revolution. Burning of fossil fuels has released large amounts of ^{14}C-absent CO_2 that has diluted the ^{14}C concentration in the atmosphere, thereby decreasing the amount of ^{14}C incorporated by organisms. Testing of nuclear devices, on the other hand, has added significant amounts of ^{14}C to the atmosphere since about 1945.

Example 10–3: Calculation of the maximum ^{14}C age of a wooden carving, given that measured ^{14}C activity of the wood is 12.37 dpm g^{-1} of C

As mentioned above, $[A_0]$ = 13.56 dpm g^{-1} of C; given, $[A_t]$ = 12.37 dpm g^{-1} of C. Substituting for $[A_0]$ and $[A_t]$ in equation (10.53),

$$t\ (\text{yr}) = 19.035 \times 10^3 \log \frac{[A]_0}{[A]_t} = 19.035 \times 10^3 \log \frac{13.56}{12.37}$$
$$= 760\ [= 19.035 \times 10^3 \log(1.096)$$
$$= 19.035 \times 10^3 \times 0.0399 = 0.76 \times 10^3 = 760]$$

Since wood for the carving could not have been obtained before the death of the source tree, the maximum age of the carving is 760 years.

10.4 Isotope ratios as petrogenetic indicators

The usefulness of radiogenic isotopes in the petrogenetic interpretation of igneous rocks lies in the fact that the isotopes of an element, because of their geochemical coherence, are not fractionated during crystal–liquid equilibria such as partial melting of source rocks or crystallization of magma. Thus,

magma generated by partial melting inherits the isotopic composition of its source as its own initial composition and, assuming no contamination due to interaction with isotopically distinct wall rocks or other batches of magma, passes on this initial isotopic composition to the products as the magma crystallizes. Such products would have the same initial ratio as the source but different present-day ratios depending on their age. It follows that the isotopic characteristics of mantle source regions can be inferred from studies of uncontaminated oceanic volcanic rocks. Conversely, it should be possible to estimate the degree of contamination experienced by a suite of igneous rocks if we know the isotopic composition(s) of the source as well as that of the contaminant(s) (DePaolo, 1981; Powell, 1984).

10.4.1 Strontium isotope ratios

Papanastassiou and Wasserburg (1969) analyzed seven basaltic achondrites (stony meteorites) and established an isochron that gave a model age of 4.39 ± 0.26 Ga (using the old value of $\lambda_{Rb} = 1.39 \times 10^{-11}\,yr^{-1}$) and an initial $^{87}Sr/^{86}Sr$ ratio of 0.69899 ± 0.00005, which they referred to as *Basaltic Achondrite Best Initial* (BABI). The basaltic achondrites are appropriate samples for this purpose for two reasons: they seem to have crystallized from silicate melts like terrestrial igneous rocks; and their extremely low Rb/Sr ratios suggest that their $^{87}Sr/^{86}Sr$ ratios have remained practically unchanged since crystallization. Subsequent studies have shown that most stony meteorites formed within the relatively narrow time interval of 4.5 ± 0.1 Ga, and the BABI value should be adjusted to 0.69897 ± 0.00003. Thus, we can conclude that the Earth was born 4.5 ± 0.1 Ga ago with a primordial $^{87}Sr/^{86}Sr$ ratio of approximately 0.699; this is now accepted as the $^{87}Sr/^{86}Sr$ ratio for a hypothetical "uniform reservoir" (UR) of planetary material from which the Earth's mantle and all its derivative products were formed.

The BABI value of 0.699 provides a reference point for tracing the evolution of terrestrial Rb–Sr systems. Sometime after its birth, the Earth developed an inhomogeneous continental crust (see section 12.2.3) that was dominated by granitic rocks enriched in Rb (which substitutes easily for K in silicate minerals), whereas Sr (which substitutes easily for Ca in silicate and carbonate minerals) was preferentially retained in the residual, depleted mantle. Consequently, crustal rocks have evolved with elevated Rb/Sr ratios and have developed much higher present-day $^{87}Sr/^{86}Sr$ ratios, whereas the depleted mantle (i.e., depleted in Rb/Sr ratio) has evolved with much lower Rb/Sr ratios and is characterized by much lower $^{87}Sr/^{86}Sr$ ratios (Fig. 10.14a). This difference allows us to use initial $^{87}Sr/^{86}Sr$ ratios to discriminate between mantle and crustal components in igneous rocks.

The present-day $^{87}Sr/^{86}Sr$ ratios of the mantle, as inferred from analyses of young oceanic basalts and large gabbroic intrusives, which are believed to have originated in the mantle and not experienced significant crustal contamination, lie in the range of 0.702 to 0.706 (Fig. 10.15), with an average of about 0.704 ± 0.002, indicating that the mantle is not entirely homogeneous. It can be calculated that to produce a ratio of 0.704 from the BABI value of 0.699 over 4.55 billion years (the Earth's age) would require an average Rb/Sr ratio of 0.027. The Rb/Sr ratio of the mantle must have decreased as a function of time because of preferential enrichment of Rb in the partial melts extracted from the mantle, and a reasonable estimate of the $^{87}Sr/^{86}Sr$ ratio of the mantle at any time in the past can be obtained by linear interpolation between 0.699 and 0.704. The evolution of strontium isotopes in continental crust is more complicated because of its heterogeneity in terms of the ages and Rb/Sr ratios of crustal rocks, but rocks having initial $^{87}Sr/^{86}Sr$ ratios greater than 0.706 indicate a crustal component.

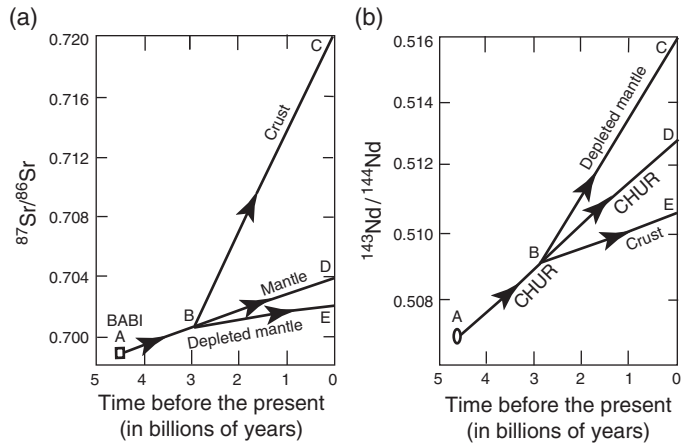

Fig. 10.14 (a) Evolution of terrestrial $^{87}Sr/^{86}Sr$ ratio over geologic time. Line ABD represents the hypothetical, closed-system evolution of mantle material, with Rb/Sr ratio of 0.027, to a present $^{87}Sr/^{86}Sr$ ratio of 0.702; in reality, this should be a slightly convex-upward curve because of the time-dependent decrease in the Rb/Sr of the upper mantle due to extraction of crustal material by partial melting. Line BC represents the closed-system evolution of a batch of crustal material with a Rb/Sr ratio of 0.15, extracted from the mantle 2.9 Ga. Line BE represents the evolution of the depleted mantle, depleted in Rb/Sr ratio resulting from extraction of the crustal material. (b) Evolution of terrestrial $^{143}Nd/^{144}Nd$ ratio over geologic time. Point A represents a $^{143}Nd/^{144}Nd$ ratio of 0.5066 for a hypothetical chondritic uniform reservoir (CHUR) 4.6 Ga. . Line ABD represents the hypothetical, closed-system evolution of the mantle material to a present $^{143}Nd/^{144}Nd$ ratio of 0.5126. Line BC represents closed-system evolution of a batch of crustal material extracted from the mantle by partial melting 2.9 Ga. Line BE represents the evolution of the depleted mantle, depleted in Sm/Nd ratio resulting from extraction of the crustal material.

10.4.2 Neodymium isotope ratios

Compared with Sr, the rare-earth elements, including Sm and Nd, are relatively immobile during postdepositional alteration (Banner, 2004). As a result, Nd isotope ratios in rocks are likely to be modified less than Sr isotope ratios in the same rocks.

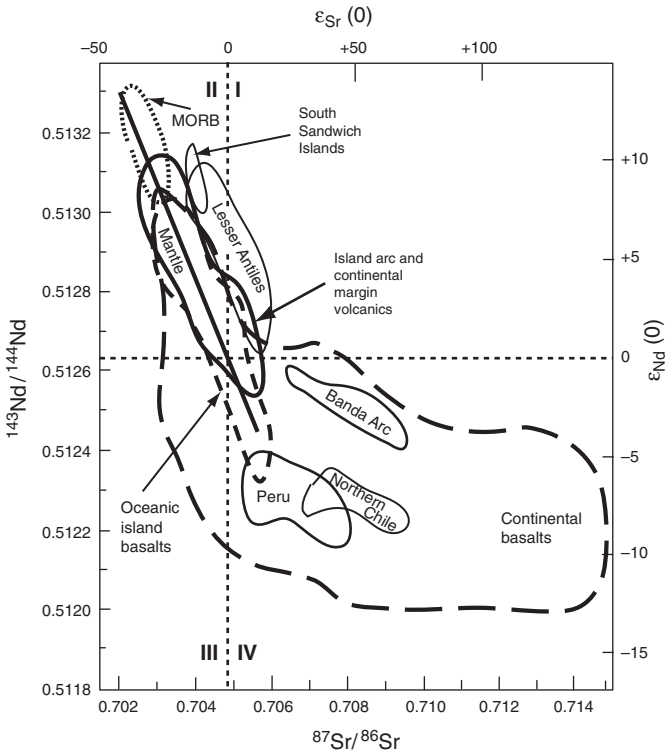

Fig. 10.15 Nd and Sr isotope compositional fields of young oceanic basalts (MORB and OIB), subduction-related basalts (island arcs formed by subduction of oceanic crust under oceanic lithosphere and continental margins adjacent to subduction zones), and continents (intraplate continental flood basalts and continental rift zone basalts). The elevated $^{87}Sr/^{86}Sr$ ratios of island arc basalts from the Lesser Antilles and the South Sandwich Islands are due to Sr contamination arising from interaction with seawater. The relatively higher $^{87}Sr/^{86}Sr$ ratios and lower $^{143}Nd/^{144}Nd$ ratios of basalts and andesites from Peru, North Chile, and the Banda Arc (Indonesia) are due to Sr and Nd contamination from crustal rocks. (Source of data: compilation by Faure (1986) from published literature.)

Chondritic meteorites, primitive planetary objects composed of condensates from the solar nebula, are considered to be the building blocks from which terrestrial planets were constructed. The terrestrial evolution of Nd isotopes is described in terms of an initial "chondritic uniform reservoir" (CHUR; DePaolo and Wasserburg, 1976) whose Sm/Nd ratio = 0.31 and whose Nd isotope ratios were uniform and the same as those of chondrites. Because the chondrites have not been affected by magmatic processes, they provide an estimate of the bulk-earth values of Sm/Nd and $^{143}Nd/^{144}Nd$. From analysis of several chondrites and an achondrite, Jacobsen and Wasserburg (1980) determined an isochron age of 4.6 Ga for the meteorites and an initial $^{143}Nd/^{144}Nd$ ratio of 0.505828 ± 0.000009 for CHUR (or 0.506609 ± 0.000008 when normalized to a $^{146}Nd/^{144}Nd$ ratio of 0.7219). The present-day values of the $^{143}Nd/^{144}Nd$ ratio (relative to a $^{146}Nd/^{144}Nd$ ratio of 0.7219) and the $^{147}Sm/^{144}Nd$ ratio of CHUR are 0.512638 and 0.1967, respectively, based on analyses of stony meteorites. The $^{143}Nd/^{144}Nd$ ratio of CHUR at any other time t (years before the present) can be calculated using the equation

$$\left(\frac{^{143}\mathrm{Nd}}{^{144}\mathrm{Nd}}\right)_{t\ (\mathrm{CHUR})} = \left(\frac{^{143}\mathrm{Nd}}{^{144}\mathrm{Nd}}\right)_{0\ (\mathrm{CHUR})} - \left(\frac{^{147}\mathrm{Sm}}{^{144}\mathrm{Nd}}\right)_{0\ (\mathrm{CHUR})} \left(e^{\lambda_{\mathrm{Sm}} t} - 1\right) \tag{10.54}$$

where $(^{143}Nd/^{144}Nd)_{t\ (CHUR)}$ is the value of this ratio in CHUR at time t in the geologic past (and would be the initial ratio of a rock derived from CHUR at time t), $(^{143}Nd/^{144}Nd)_{0\ (CHUR)}$ is the present-day value of this ratio in CHUR (= 0.512638), and $(^{147}Sm/^{144}Nd)_{0\ (CHUR)}$ is the value of this ratio in CHUR at the present time (= 0.1967).

The terrestrial evolution of the $^{143}Nd/^{144}Nd$ ratio from its CHUR value of 0.505828 at 4.6 Ga (Fig. 10.14b) is analogous to that of the $^{87}Sr/^{86}Sr$ ratio from its BABI value of 0.699 in UR. The $^{143}Nd/^{144}Nd$ ratio has increased as a function of the duration of ^{147}Sm decay, both in the bulk earth and in its differentiated products, but at a faster rate in the depleted mantle compared with the continental crust. The higher enrichment of ^{143}Nd in the depleted mantle is because of preferential partitioning of Nd, relative to Sm, into felsic differentiates. As a result, compared with the depleted mantle (with an elevated Sm/Nd ratio), the crust has evolved with lower Sm/Nd ratios and developed significantly lower present-day $^{143}Nd/^{144}Nd$ ratios. This difference allows us to use initial $^{143}Nd/^{144}Nd$ ratios to discriminate between mantle and crustal components in igneous rocks. If the initial $^{143}Nd/^{144}Nd$ ratio for a cogenetic igneous suite is significantly higher than the corresponding $^{143}Nd/^{144}Nd$ ratio of CHUR at the time of crystallization of the rocks, the magma most probably was derived by partial melting of the mantle; if the initial ratio is significantly lower, the magma most probably had a crustal source or at least a crustal component. Note that interpretations based on high and low initial $^{87}Sr/^{86}Sr$ ratios are just the opposite.

10.4.3 *Combination of strontium and neodymium isotope ratios*

A combination of Nd and Sr isotope ratios provide a better appreciation of the constraints on petrogenesis of igneous rocks and the heterogeneity of the mantle as reflected by the isotopic composition of magmas generated in the mantle. The variation in measured $^{207}Pb/^{204}Pb$ and $^{206}Pb/^{204}Pb$ ratios of young oceanic basalts also attest to the heterogeneity of the mantle (Wilson, 1989).

In general, differences in the Nd isotope ratios between the rocks of interest and CHUR are quite small, and it is convenient to represent the comparison by the "epsilon parameter" introduced by DePaolo and Wasserburg (1976):

$$\varepsilon_{\mathrm{Nd}} = \left[\frac{(^{143}\mathrm{Nd}/^{144}\mathrm{Nd})_{\mathrm{meas}}}{(^{143}\mathrm{Nd}/^{144}\mathrm{Nd})_{\mathrm{p\ (CHUR)}}} - 1\right] \times 10^4 \tag{10.55}$$

where $(^{143}Nd/^{144}Nd)_{meas}$ is the measured value of this ratio in a sample and $(^{143}Nd/^{144}Nd)_{p\ (CHUR)}$ the present value of this ratio in CHUR (= 0.512638, normalized to $^{146}Nd/^{144}Nd$ = 0.7219). Calculation of this parameter by normalization of all data to CHUR also circumvents the problem of different normalization procedures followed by different laboratories. We often consider ε_{Nd} values together with ε_{Sr} values, the latter defined in an analogous way as

$$\varepsilon_{Sr} = \left[\frac{(^{87}Sr/^{86}Sr)_{meas}}{(^{87}Sr/^{86}Sr)_{p\ (UR)}} - 1 \right] \times 10^4 \qquad (10.56)$$

where UR represents "uniform reservoir", equivalent to bulk earth, and $(^{87}Sr/^{86}Sr)_{p\ (UR)}$ is the present value of this ratio in the uniform reservoir (= 0.7045). The bulk earth reference reservoir for Sr, however, is not well defined (White and Hofmann, 1982), and many authors prefer to use measured $^{87}Sr/^{86}Sr$ ratios instead of calculated ε_{Sr} values.

A value of zero for either ε_{Nd} or ε_{Sr} would indicate that the corresponding measured isotopic ratio of the igneous rock is same as that of the CHUR or UR at present. A positive ε_{Nd} value implies that the magma was derived from a depleted mantle source; a negative ε_{Nd} value implies that the magma was derived from, or contaminated by, a source with a lower Sm/Nd ratio, such as old crustal material that had separated from CHUR (see Fig. 10.14a). The implications of positive and negative ε_{Sr} values are just the opposite of each other; for example, a crustal source of magma or its contamination by a crustal source is indicated by positive ε_{Sr} values (see Fig. 10.14b).

Figure 10.15 is a plot of measured $^{87}Sr/^{86}Sr$ versus $^{143}Nd/^{144}Nd$ ratios of selected young oceanic, subduction-related, and continental basalts. The most conspicuous feature of the plot is the negative correlation between ε_{Nd} and ε_{Sr} for mid-oceanic ridge basalts (MORBs) and oceanic island basalts (OIBs), often referred to as the *Mantle Array*. The MORBs and most of the OIBs fall in quadrant II of this plot ($\varepsilon_{Nd} > 0$, $\varepsilon_{Sr} < 0$) and are interpreted to have originated from "depleted" mantle sources having higher Sm/Nd ratios than CHUR and lower Rb/Sr ratios than UR (see Fig. 10.14). Some OIBs, however, plot in quadrant IV ($\varepsilon_{Nd} < 0$, $\varepsilon_{Sr} > 0$), indicating the presence of "enriched" magma sources (i.e., with lower Sm/Nd ratios than CHUR and higher Rb/Sr ratios than UR) in the mantle under the ocean basins. The wide range of Nd and Sr isotope ratios marking the Mantle Array has been interpreted variously as the result of mixing of magmas from "depleted" and "enriched" sources (DePaolo and Wasserburg, 1979), partial melting of a heterogeneous mantle source (Zindler *et al.*, 1979), incorporation of subducted oceanic or continental crust into the magma (Hawkesworth *et al.*, 1979a), and magma generation by disequilibrium melting of a mantle with variable phlogopite contents (Flower *et al.*, 1975). A detailed discussion of the isotopic characteristics of oceanic basalts is given by Cousens and Ludden (1991).

Volcanic rocks from island arcs (resulting from subduction of oceanic crust under oceanic lithosphere) plot largely in quadrant II along the Mantle Array, but their lower Nd and Sr ratios are not consistent with magmas formed by remelting of an oceanic crust composed only of MORBs. Volcanic rocks from continental margins, such as those from South America, plot in quadrant IV; these rocks represent magmatic activity resulting from subduction of oceanic crust under continental crust and contamination with Nd and Sr derived from felsic crustal rocks. As expected, crustal contamination is more pronounced in the case of continental basalts. Some continental basalts, however, plot in quadrant II, and may represent sources under the continent similar to those for OIBs.

The paucity of rocks falling in quadrant I ($\varepsilon_{Nd} > 0$, $\varepsilon_{Sr} > 0$) and in quadrant III ($\varepsilon_{Nd} < 0$, $\varepsilon_{Sr} < 0$) is to be expected because simultaneous enrichment or depletion of both Nd and Sr is incompatible with their geochemical behavior. The Sr enrichment in some of the Lesser Antilles rocks is most likely due to seawater contamination (Hawkesworth *et al.*, 1979b) and the unusual Nd and Sr of some continental basalts (such as the Tertiary volcanic province of northwest Scotland) plotting in quadrant III is believed to be due to contamination from basement granulites (Carter *et al.*, 1978).

10.4.4 Osmium isotope ratios

The Re–Os system is unique compared to Rb–Sr, U–Pb, and Sm–Nd systems for which all parent–daughter pairs are incompatible in mantle phases, whereas Re and Os display marked fractionation between mantle and crustal systems. Osmium is a highly compatible element in mantle phases, and is strongly retained in the mantle during most magmatic processes that produce crust from mantle. Rhenium, on the other hand, is an incompatible element in mantle phases ($K_{D(Re)} < 0.01$; Walker *et al.*, 1988) and readily partitioned into crustal material relative to Os. The recycling of crustal material into the mantle may complicate the interpretation of intramantle processes when using other isotopic systems. The Re–Os sysem, when used together with other isotopic systems may provide a unique insight into the evolution of the mantle and the crust over geologic time. The Re–Os sysem in the mantle is likely to have been insensitive to the incorporation of crustal material because of the similar Re abundances and much lower Os abundances in the crust relative to the mantle (Walker *et al.*, 1988).

Because of the decay of ^{187}Re, which is preferentially partitioned into the crust, the crustal osmium is more radiogenic compared to that in the mantle, the $^{187}Os/^{186}Os$ ratio increasing with decreasing geologic age. Thus, osmium isotopic composition is a powerful tracer of crustal contaminaton of mantle-derived magmas. For example, the inhomogeneity of the initial $^{187}Os/^{186}Os$ ratio (ranging from the mantle value of 0.9 corresponding to an age of 2.66 Ga to as high as 1.15) for chromite bands in the

Stillwater Layered Complex in Montana has been interpreted to reflect contamination of mantle-derived mafic magmas by an enriched crustal compoent (Lambert *et al*., 1989). The high $^{187}Os/^{186}Os$ ratios of laurite from chromitite units (UG1 and UG2) and the Merensky Reef of the Rustenburg Layered Suite (2.05 Ga), Bushveld Complex (Fig. 10.12b), may also be due to a large crustal component in the related magma (McCandless and Ruiz, 1991). Alternatively, the high radiogenic osmium may be indicative of a hydrothermal origin of the Mrensky PGE ore, as proposed by many authors (see, e.g., Boudreau and McCallum, 1986). Crustal contamination increases the activity of SiO_2 in a mafic magma, and thereby decreases the solubility of sulfur in the magma (Haughton *et al*., 1974). This is an important consideration for the formation of Ni–Cu sulfide deposits hosted in mafic–ultramafic igneous bodies.

10.5 Summary

1. Radioactivity is the phenomenon of spontaneous decay of unstable nuclides, which are referred to as radionuclides. Radioactive decay occurs by three mechanisms: beta decay – emission of a negatively charged beta particle (β^-), or emission of a positively charged beta particle (β^+), or electron capture; alpha decay, emission of an alpha particle (α^{2+}) composed of two neutrons and two protons; and spontaneous nuclear fission, involving the break up of the nucleus and release of a large amount of energy.
2. The rate of radioactive decay is written as:

$$-\frac{dN}{dt} = \lambda N$$

where N denotes the number of parent atoms remaining at any time t, and λ is the *decay constant* (expressed in units of reciprocal time), which is characteristic for a particular radionuclide and is assumed to have remained constant during Earth's history.

3. The decay constant is related to the half-life ($t_{1/2}$) of the decay process by the equation:

$$\boxed{t_{1/2} = \frac{0.693}{\lambda}}$$

4. Radiogenic isotopes, isotopes produced by radioactive decay of radionuclides, have wide application to geochronology, mantle evolution, igneous petrogenesis, chemical stratigraphy, provenance studies, and the study of temporal changes in Earth surface processes.
5. The basic general equation used for age determination of rocks and minerals in closed systems is:

$$D = D_0 + N\,(e^{\lambda t} - 1)$$

where D and D_0, respectively, are the total number of daughter atoms after time t and the number of daughter atoms present initially per unit weight of the sample. The equation for Rb–Sr dating is:

$$\boxed{\frac{^{87}Sr}{^{86}Sr} = \left(\frac{^{87}Sr}{^{86}Sr}\right)_0 + \frac{^{87}Rb}{^{86}Sr}\,(e^{\lambda_{Rb}t} - 1)}$$

A plot of $^{87}Sr/^{86}Sr$ (y axis) against $^{87}Rb/^{86}Sr$ (x axis) for a suite of comagmatic samples will ideally define a straight line, an isochron, with the y-axis intercept = $(^{87}Sr/^{86}Sr)_0$, the initial ratio, and slope (m) = $e^{\lambda_{Rb}t} - 1$ from which we can calculate t. The isochron method of age determination for other systems, such as ^{147}Sm / ^{143}Nd, ^{176}Lu / ^{176}Hf ^{187}Re / ^{187}Os, and ^{40}K / ^{40}Ar, is based on the same principles and equations of the same form.

6. Three widely used approaches for geochronology based on U–Th–Pb systems are: (i) the U–Pb concordia diagram, which is useful for providing age information in spite of lead loss from the system; (ii) the "207–206 date," which does not depend on the present-day U content of the sample and, therefore, is not affected by recent loss of U; and (iii) the common lead method, which is particularly suitable for dating sulfide deposits.
7. The ^{40}Ar–^{39}Ar method of geochronology involves the conversion of a known fraction of the $^{39}_{19}K$ in a K-bearing sample to $^{39}_{18}Ar$ by irradiation with fast neutrons in a nuclear reactor, and then measuring the $^{40}Ar^*/^{39}Ar$ ratio in the gas released by heating the sample to fusion either in one step or in several incremental steps.
8. A method used for dating relatively young (<70,000 years) samples containing biogenic carbon is based on the decay of ^{14}C (half-life = 5730 ± 40 yr):

$$\boxed{t = \frac{1}{\lambda_{C-14}} \ln \frac{[A]_0}{[A]_t} = 19.035 \times 10^3 \log \frac{[A]_0}{[A]_t}}$$

where $[A]_t$ is the concentration of ^{14}C in a sample in equilibrium with the atmosphere and $[A]_0$ the concentration of ^{14}C in the same sample at the time of death of the animal or plant (commonly referred to as specific activities of ^{14}C).

9. Sr and Nd isotopes provide insight into the evolution of the mantle and genesis of igneous rocks because the isotopes, owing to their geochemical coherence, are not fractionated during crystal–liquid equilibria such as partial melting or magma crystallization processes.
10. The mantle evolution curve for osmium isotopes is very useful for assessing crustal contamination of mantle-derived magmas of known age. The mantle evolution curve can also be used for age determination

just from measured $^{187}Os/^{186}Os$ ratios of Os-rich samples such as osmiridium and laurite ($^{187}Os/^{186}Os = 1.040 - 0.050768\ t$).

10.6 Recapitulation

Terms and concepts

Alpha decay
Anomalous lead
Basaltic achondrite best initial (BABI)
Beta decay
Blocking temperature
Branched decay
Chondritic uniform reservoir (CHUR)
Common lead
Concordant dates
Concordia
Cosmogenic nuclides
Daughter (product)
Decay constant
Decay series
Depleted mantle
Discordia
Electron capture
Epsilon parameters (ε_{Nd}, ε_{Sr})
Excess argon
Geochron
Geochronology
Half-life
Initial ratio
Isochron
Mantle Array
Model age
Nuclear fission
Ordinary lead
Primordial lead
Radioactivity
Radioisotope
Radionuclide
Single-stage lead
Uniform reservoir (UR)

Computation techniques

- Calculation of age using geochronologic equations for various systems.
- Graphical techniques for determination of geologic age and intial ratios.
- Construction of concordia diagrams.
- Construction of single-stage growth curves and isochrons for lead isotopes.
- Construction of $^{40}Ar/^{39}Ar$ age spectrum diagram.

10.7 Questions

The relevant decay constants are as listed in Table 10.2. The use of spreadsheets, as in the computer program Excel, is strongly recommended.

1. Show that the decay constant (λ) for a radionuclide is related to its half-life ($t_{1/2}$) by the equation:

$$t_{1/2}(\text{years}) = \frac{0.693}{\lambda\ (y^{-1})}$$

2. The isotope ^{176}Lu undergoes β^- decay to ^{176}Hf with a long half-life. From a plot of $^{176}Hf/^{177}Hf$ (y axis) versus $^{176}Lu/^{177}Hf$ (x axis) for a suite of meteorites (eucrites), Patchett and Tatsumoto (1980) obtained a 10-point isochron with a slope of 0.0934 and an initial $^{176}Hf/^{177}Hf$ ratio of 0.27973. The age of the meteorites is known to be 4550 Ma. Calculate the half-life of ^{176}Lu decay.
3. How many half-lives would it take for a given population of plutonium atoms ($^{239}_{94}Pu$) to be reduced to less than 0.1% of the original? Half-life of $^{239}_{94}Pu = 2.44 \times 10^4$ yr.
4. Calculate the $^{147}Sm/^{144}Nd$ ratio of a rock containing 1.83 ppm Sm and 5.51 ppm Nd. The atomic weight of Sm is 150.36 and that of Nd is 144.24. The isotopic percentage abundance of ^{147}Sm is 15.0 and that of ^{144}Nd is 23.954.
5. For a sample of volcanic rock, the measured lead isotope ratios are as follows:

$$^{204}Pb/^{206}Pb = 0.143;\ ^{206}Pb/^{206}Pb = 1.000;\ ^{207}Pb/^{206}Pb = 12.95;\ \text{and}\ ^{208}Pb/^{206}Pb = 21.96.$$

   Recalculate the abundance of the ratios in terms of atom percent and calculate the atomic weight of lead in this sample (Faure, 1986, p. 304). The masses of the isotopes (in amu) are:

   $^{204}Pb = 203.970$; $^{206}Pb = 205.9744$; $^{207}Pb = 206.9759$; and $^{208}Pb = 207.9766$.

6. Determine the model age and the initial ratio of the Sudbury Nickel Irruptive norite by constructing an isochron diagram using the whole-rock Rb–Sr isotope ratios given below (Gibbins and McNutt, 1975). What is the initial ratio and what is its significance?

Sample	$^{87}Rb/^{86}Sr$	$^{87}Sr/^{86}Sr$	Sample	$^{87}Rb/^{86}Sr$	$^{87}Sr/^{86}Sr$
W101	0.3243	0.7155	W118	0.1129	0.7097
W102	0.3852	0.7172	W120	0.1213	0.7098
W103	0.3736	0.7173	W124	0.2259	0.7129
W104	0.4228	0.7181	W129	0.3212	0.7153
W110	0.2953	0.7144	W134	0.2866	0.7143
W113	0.2374	0.7129	W136	0.3011	0.7148
W116	0.1158	0.7100			

7. The Sm–Nd isotopic data given below are for samples of mafic–ultramafic lavas from the Norseman–Wiluna greenstone belt in the Kambalda area, Western Australia (Claoué-Long *et al.*, 1984).

Sample	$^{147}Sm/^{144}Nd$	$^{143}Nd/^{144}Nd$	Sample	$^{147}Sm/^{144}Nd$	$^{143}Nd/^{144}Nd$
1	0.1436	0.511610	7	0.2592	0.514110
2	0.1804	0.512413	8	0.2034	0.512997
3	0.1520	0.511832	9	0.2053	0.512942
4	0.1923	0.512634	10	0.1976	0.512762
5	0.2254	0.513375	11	0.2002	0.512843
6	0.2352	0.513601			

Fit the data to an isochron by least-squares regression, determine the initial $^{143}Nd/^{144}Nd$ ratio from the graph, and calculate the age based on the slope of the regression line. What is the significance of the initial ratio for this suite of lavas?

8. The Rb–Sr data given below are for whole-rock samples from amphibolite metamorphic facies of the Lewisian gneiss complex in Scotland (Moorbath *et al.*, 1975), and the Sm-Nd data are for whole-rock samples from granulite metamorphic facies of the same complex (Hamilton *et al.*, 1979). Do the data yield concordant Rb–Sr and Sm–Nd dates for the complex? If not, suggest a reasonable explanation for the discordance. Assuming that the complex is of igneous origin, what can you say about the source region for the magma from the initial ratios?

Sample	$^{87}Rb/^{86}Sr$	$^{87}Sr/^{86}Sr$	Sample	$^{147}Sm/^{144}Nd$	$^{143}Nd/^{144}Nd$
1	0.133	0.7085	1	0.1960	0.512756
2	0.177	0.7090	2	0.2346	0.513518
3	0.086	0.7040	3	0.1707	0.512195
4	0.240	0.7107	4	0.1082	0.511006
5	0.501	0.7211	5	0.0741	0.510376
6	0.594	0.7224	6	0.0875	0.510634
7	0.191	0.7096	7	0.1030	0.510962
8	0.104	0.7049	8	0.0775	0.510501
9	0.400	0.7153	9	0.1127	0.511143
10	1.710	0.7668	10	0.0871	0.510638
11	0.368	0.7152	11	0.0999	0.510902
12	0.049	0.7032			
13	0.298	0.7132			

9. Listed below is a set of measured lead–uranium isotope ratios for a suite of monazite and uraninite samples from Zimbabwe (Rhodesia) as reported by Ahrens (1955b):

Sample	$^{206}Pb^*/^{238}U$	$^{207}Pb^*/^{235}U$
(1) Monazite (Manitoba)	0.634	14.75
(2) Monazite (Ebonite)	0.507	12.45
(3) Monazite (Jack Tin)	0.420	10.10
(4) Monazite (Irumi)	0.383	9.02
(5) Uraninite (Manitoba)	0.270	5.85
(6) Monazite (Antsirabe)	0.241	5.16

Plot a concordia diagram for this suite of samples. What is a reasonable interpretation of the concordia diagram? What are the assumptions for your interpretation?

10. Calculate the "^{207}Pb–^{206}Pb age" of the Lake Johnston batholith in the Kalgoorlie–Norseman area, Western Australia from the measured $^{206}Pb/^{204}Pb$ and $^{206}Pb/^{204}Pb$ ratios of K-feldspar (K-fe), plagioclase (Plag) and whole-rock (WR) samples listed below (Oversby, 1975):

Sample	$^{206}Pb/^{204}Pb$	$^{207}Pb/^{204}Pb$	Sample	$^{206}Pb/^{204}Pb$	$^{207}Pb/^{204}Pb$
1 (K-fe)	14.437	15.121	7 (Plag)	23.202	16.674
2 (K-fe)	15.321	15.238	8 (Plag)	20.958	16.233
3 (K-fe)	14.319	15.079	9 (WR)	29.003	17.696
4 (K-fe)	15.196	15.275	10 (WR)	28.106	17.497
5 (K-fe)	16.519	15.445	11 (WR)	29.230	17.772
6 (K-fe)	15.330	15.256	12 (WR)	24.172	16.829

11. A sample of galena from a sulfide deposit has the following isotopic composition: $^{206}Pb/^{204}Pb = 14.97$; $^{207}Pb/^{204}Pb = 15.30$; and $^{208}Pb/^{204}Pb = 34.82$. Calculate the model age and the $^{238}U/^{204}Pb$ ratio (μ) of the source region of the lead, using the single-stage Holmes–Houtermans model of lead evolution and the values of the parameters as given in the text. How would you test if the Pb actually had a single-stage history?

12. Construct a single-stage growth curve for common lead in $^{206}Pb/^{204}Pb$ (x axis) – $^{207}Pb/^{204}Pb$ (y axis) space, using the values of a_0, b_0, λ_{238}, and λ_{238} as given in the text. Assume $\mu = 10$. Interpret the lead isotopic data (Brown, 1969) given below for samples of galena from an ore deposit in southeast Missouri.

Sample	$^{206}Pb/^{204}Pb$	$^{207}Pb/^{204}Pb$	Sample	$^{206}Pb/^{204}Pb$	$^{207}Pb/^{204}Pb$
1	20.15	15.79	8	20.72	15.94
2	20.34	15.87	9	20.87	15.96
3	20.41	15.92	10	20.96	15.99
4	20.82	15.93	11	20.80	15.96
5	20.81	15.91	12	20.90	15.96
6	20.76	15.99	13	21.08	16.07
7	20.79	15.97	14	21.33	16.06

13. Analyses of volcanic rock samples from McLennans Hills yielded the following K–Ar isotope ratios (McDougall *et al.*, 1969):
Determine the age and initial ratio of the volcanic suite using an isochron plot. How much excess argon does this suite contain?

Sample	$^{40}Ar/^{36}Ar$	$^{40}K/^{36}Ar$ ($\times 10^6$)	Sample	$^{40}Ar/^{36}Ar$	$^{40}K/^{36}Ar$ ($\times 10^6$)
1	331.83	5.483	6	297.52	0.856
2	335.57	5.533	7	309.96	4.222
3	318.12	4.317	8	319.81	4.112
4	342.38	7.642	9	338.95	6.980
5	347.02	8.454			

14. The data listed below pertains to the $^{40}Ar-^{39}Ar$ dating of Apollo 15 lunar anorthosite rock 15415,9 by the incremental heating method (Husian *et al.*, 1972). Calculate the apparent age for each heating step and determine the "plateau age" of the sample from the appropriate graph. For this problem, $J = 0.0983$.

Temperature (°C)	Cumulative fraction ^{39}Ar	Radiogenic $^{40}Ar/^{39}Ar$	Temperature (°C)	Cumulative fraction ^{39}Ar	Radiogenic $^{40}Ar/^{39}Ar$
800	0.03	58.14	1500	0.79	83.32
900	0.10	61.34	1650	1.00	79.80
1000	0.27	72.77	800 – 1650	1.00	77.20
1200	0.61	80.15	1000 – 1650	0.90	79.00

15. The specific ^{14}C activity of a sample of charcoal is determined to be 12.47 dpm g^{-1} of carbon. What is the age of the sample if the initial activity of ^{14}C in this sample was 13.56 dpm g^{-1} of carbon? What would be the error if the initial activity were 15.30 dpm g^{-1} of carbon?
16. The Sr and Nd isotopic data for the young (< 1 Ma) basaltic rocks of the Azores Islands (Atlantic Ocean) presented below are from the compilation by White and Hofmann (1982). SM = Sao Miguel Island; F = Faial Island.

Sample	$^{87}Sr/^{86}Sr$	$^{143}Nd/^{144}Nd$	Sample	$^{87}Sr/^{86}Sr$	$^{143}Nd/^{144}Nd$
SM-2a	0.70337	0.512926	F- 2	0.70386	0.512871
SM-12	0.70514	0.512707	F-14	0.70394	0.512870
SM- 6	0.70430	0.512812	F-21	0.70384	0.512943
SM- 6	0.70429	0.512810	F-29	0.70392	0.512877
SM-28	0.70525	0.512732	F-33	0.70393	0.512843

Construct a ε_{Sr} (x axis) versus ε_{Nd} (y axis) plot and discuss the possible reasons for the spread of the isotopic data.